



EURASIAN JOURNAL OF
**MEDICAL AND
BIOLOGICAL SCIENCES**



Volume 3, Number 1, June, 2023

ISSN:2757-8453

Eurasian

Journal of Medical and Biological Sciences

Aims and Scope: Eurasian Journal of Medical and Biological Sciences (Eurasian J Med Biol Sci) is an international, open access periodical published in accordance with independent, unbiased, and double-blinded peer-review principles.

The journal is published as two issues per year (June and December). The journal will consider submissions from all over the world, on research works not being published or submitted for publication towards publication as full paper, review article and short communication. The publication language of the journal is English

Copyright © 2022 Eurasian Journal of Medical and Biological Sciences. No parts of publication in the Eurasian Journal of Medical and Biological Sciences may be reproduced, stored, transmitted or disseminated, in any form or by any means without prior permission from editor. Authors are responsible for all ideas in the manuscript.

Principal Contact: info@eurasianscience.com or eurasiainscience@gmail.com

The Journal has an international editorial board.

Abstracted and Indexed in:

Google Scholar
Indexcopernius index
Academic Researches Index
Advanced Sciences Index
Cite Factor
Asos Indeks

Volume 3, Number 1, June 2023

Web: <http://eurasianscience.com/>
<http://eurasianscience.com/index.php/ejmb/issue/view/5>

Email: info@eurasianscience.com
eurasianscience@gmail.com

Editor-in-Chiefs

Dr. Falah Saleh Mohammed
Dr. Nady Braidy
Dr. Zeliha Selamoglu

Editorial Director

Dr. Mustafa Sevindik

Statistics and Language Editors

Dr. Demet Çanga Dr. Ömer Lekesiz

Layout Editors

Dr. Ali İmran Korkmaz Dr. Mürşit Ömür Koyuncu

Editorial Board

Dr. Adnan Ayan	Dr. Kamala Badalova
Dr. Alamgir Khan	Dr. Maria Daglia
Dr. Ali Raza Memon	Dr. Md Amjad Beg
Dr. Alpaslan Dayangaç	Dr. Mehmet Yaran
Dr. Antoni Sureda	Dr. Muhittin Doğan
Dr. Ardalan Pasdaran	Dr. Muhammad Babar TAJ
Dr. Arshad Javaid	Dr. Muhammad Ajmal Shah
Dr. Aydın Atakan	Dr. Muhammed Dogan
Dr. Azhar Rasul	Dr. Mustafa Pehlivan
Dr. Betül Ozdemir	Dr. Nazmi Polat
Dr. Burak Bircan	Dr. Nuh Korkmaz
Dr. Bülent Ünver	Dr. Omar Al-Habib
Dr. Dariush Ilghari	Dr. Nouredine Djebel
Dr. Ebrahim Alinia-Ahandani	Dr. Ramin Ekhteiari Salmas
Dr. Eduardo Sobarzo-Sanchez	Dr. Rosa Maria Orriols
Dr. Emre Sevindik	Dr. Rzgar Farooq Rashid
Dr. Ergin Şahin	Dr. Sachchida Nand Rai
Dr. Eva Urgeova	Dr. Sachiyo Aburatani
Dr. Gulnara Azizova	Dr. Saeed Ullah Jan
Dr. Gamal Badr	Dr. Samra Mededovic
Dr. Hasan Akgül	Dr. Sevgi Durna Dastan
Dr. Hayri Baba	Dr. Sevgi Gezici
Dr. Maria Daglia	Dr. Shahid Abbas
Dr. Ilgaz Akata	Dr. Tetiana Krupodorova
Dr. İlter Demirhan	Dr. Tugay Ayasan

Volume 3, Number 1, June 2023

Web: <http://eurasianscience.com/>
<http://eurasianscience.com/index.php/ejmb/issue/view/5>
Email: info@eurasianscience.com
eurasianscience@gmail.com

Eurasian

Journal of Medical and Biological Sciences

REFEREES OF VOLUME 3, NUMBER 1, June 2023

Dr. Ahmet Aksoy
Dr. Aslı Yılmaz
Dr. Betül Özdemir
Dr. Emre Cem Eraslan
Dr. Fatih Doğan Koca
Dr. Hasan Akgül

Dr. Kemal Çetin
Dr. Murat Yabanlı
Dr. Sevgi Durna Dastan
Dr. Shereen Butti
Dr. Özlem Ünlü

Volume 3, Number 1, June 2023

Web: <http://eurasianscience.com/>
<http://eurasianscience.com/index.php/ejmbs/issue/view/5>
Email: info@eurasianscience.com
eurasianscience@gmail.com

Eurasian

Journal of Medical and Biological Sciences

Vol.3, No.1, June 2023

TABLE OF CONTENTS

REVIEW ARTICLES	Pages
A Closer Look at Some Medical Use of Green Persian Walnut Shell Sahebeh Hajipour, Ebrahim Alinia-Ahandani, Zeliha Selamoglu	1-7
Systematic Review of Cardiovascular Health Complications Associated with Oral Contraceptive Pills Alamgir Khan, Muhammad Zafar Iqbal Butt, Muhammad Jamil, Zeliha Selamoglu, Elifsena Canan Alp	8-11
MEDICAL SCIENCES	Pages
Application of Experimental Design Methodology to Optimize Azithromycin Removal by Graphene/Iron Oxide Nanocomposite Saeed Ullah Jan, Saad Melhi, Nadia Bibi, Anam Nisar, Sana Faryal, Nabeela, Tahira Naz, Amina Bibi, Aman Ullah, Zeliha Selamoglu	12-22
BIOLOGICAL SCIENCES	Pages
Comparison of heavy metal concentrations in marine macroalgae of the Northern Aegean Sea, Türkiye Fatma Koçbaş, Saniye Türk Çulha, Ayşe Gündoğdu, Neslihan Türkçü	23-33
Investigation of the antifungal activities of cryogels for potential use as wound dressing materials Koray Şarkaya, Berna Kavakçioğlu Yardımcı, Ayşenur Güler	34-40



A Closer Look at Some Medical Use of Green Persian Walnut Shell

Sahebeh Hajipour^{*1}, Ebrahim Alinia-Ahandani², Zeliha Selamoglu³

^{*1} Department of Biology, Faculty of Science, Golestan University, Golestan, Iran

² Department of Biochemistry, Payame Noor University, Tehran, Iran

³ Medical Biology Department, Nigde Ömer Halisdemir University, Turkey

Received : 05/11/2022

Revised : 04/12/2022

Accepted : 11/12/2022

ABSTRACT: Persian walnut (*Juglans regia* L) is a tree species that has been of interest to humans since its medicinal and nutritional effects. The wild population of this species has been recorded in the temperate and semi-arid mountainous regions of Central Asia, East and South Asia, the Middle East and the Caucasus region. The origin of Iran's walnut communities is in the Hyrcanian forest in the north of Iran. Walnut is a source of various medicinal compounds such as various biologically active substances such as polyphenols, flavonoids, steroids, phospholipids, triterpenes, kinins, fatty acids, tannins, gallic acid and ellagic acid, and plays an important role in medicine, especially in traditional Iranian medicine. All these compounds have turned walnut into an important commercial product that is of high value in the pharmaceutical and food industry. In this study, various medicinal effects of this valuable species such as anti-cancer, anti-oxidant and anti-diabetic effects have been investigated according to recent researches and it shows that depending on the different climatic conditions, the medicinal compounds of walnut can change and this phenomenon is necessary. It creates more research in this field.

Keywords: Hyrcanian, Anti-cancer, medicinal effects, traditional medicine, Walnut

INTRODUCTION

Juglans regia L. (Persian Walnut) is a tree species that has been of interest to humans since the past. The fruit of *J.regia* is 5 cm long with a leathery, wrinkled exocarp and a hard 4-lobed endocarp. Fruits are born in clusters. The seeds are edible. The nuts are round and measure 1.5-2 inches. Wild populations of *J. regia* have been recorded in temperate and semi-arid mountainous regions of Central Asia, East and South Asia, the Middle East, and the Caucasus region. These forests are characterized by an extraordinary morphological and physiological diversity and are home of numerous wild relatives of cultivates species, highlighting the importance as a global biodiversity hot-spot (Verma et al., 2020).

J. regia has been introduced to a much wider area in the past due to its special nutritional importance and significant economic value. Walnuts were cultivated on a commercial scale in 48 countries of the world on a total area of 647.497 hectares in 2016. Global annual walnut production was estimated at 3,763.725 metric tons (in shell) in 2016, equaling a total production value of more than USD 14 billion. China and the United States accounted for 47 and 31 percent of the total global walnut production, respectively. Further major producer countries include Chile, Iran and Ukraine (Ahandani et al., 2014; Shigavea and Darr, 2020).

The origin of Iranian walnut communities in the Hyrcanian forest in northern Iran is very complex, and more efforts are needed to protect the diverse populations of this valuable genetic resource. In modern times, it is very difficult to find remaining natural populations of Persian walnut (*J. regia*) in its native range, but natural populations of this species can still be found in Hyrcanian forests. Recent studies have listed the presence of this species in North Iran in Talesh, Astara, Dino Chal, Goli Daghi (1500 m) and Bandargaz. The distribution of this species is mostly in Golestan province, including the cities of Bandar Gaz, Zarin Gol (900 m), Rabat Gezlaq (2400 m), Mazandaran province, including Farsang Dar, Haraz Valley. (100 meters) and the mountain slopes of this province and in Gilan province near Hashtpar (60 meters) the existence of this valuable species has also been reported (6-9). Some very valuable wild cultivars were identified and named for the first time by Alinia-Ahandani et al, in Lahijan region in Guilan province in Iran, which have potential capacities in the field of moisture-resistant cultivars and also very old generations of Hyrcanian walnut in this region (Ahandani et al., 2014; Alinia-Ahandani et al., 2019).

The origin of the walnut tree is from the eastern Balkans to the Himalayas and southwestern China. Persian or common walnut (*J. regia*) is the most well-known member, found mainly in temperate regions and commercially cultivated in many parts of the world. Now the walnut trees are growing. In parts of the world, including Asia (the foothills of the Himalayas, Iran, China and Japan), southern and eastern Europe, as well as North and South America. The walnut tree grows in some other provinces of Iran, such as Fars, Hamadan, Kohgiluyeh, Boyer Ahmad and Lorestan. A species of walnut tree with the scientific name *J.*

J. regia grows in Iran. The walnut tree is sensitive to very hot and very cold weather in summer and winter. Walnut trees are single-stemmed plants with a height of about 10 to 25 meters. They have claw-shaped compound leaves. It appeared with male and female flowers separately on them. During the hibernation period, walnut trees can tolerate cold weather up to -11 degrees Celsius. The maturity of the walnut tree is directly related to various factors such as the species, race, climate and place of its growth (Aryapak and Ziarati, 2014; Habibi et al., 2022).

J. regia is a rich source of various types of chemical compounds. It plays a big role in Ayurveda and homeopathy system of medicine. It contains various biologically active substances such as polyphenols, flavonoids, steroids, phospholipids, triterpenes, kinins, fatty acids, tannins such as gallic acid and ellagic acid. Ellagic acid is responsible for anti-cancer and immunity properties. The active ingredient of *J. regia* is juglone (quinone). The bark of *J. regia* contains higher polyphenolic compounds which are responsible for antioxidant and antibacterial activities. The leaves of *J. regia* are rich in alkaloids, saponins, flavonoids, which show anti-diabetic effect. Walnut oil contains omega-3 and omega-6 unsaturated fatty acids, mono, di, triacylglycerol, free fatty acids, oleic and linoleic acids, which are beneficial for heart diseases, lowering cholesterol and blood sugar. The green husk contains juglone and polyphenols, which are used in textile dyeing industries. *J. regia* plant contains monoterpenes, sesquiterpenes, juglone, sterols, tocopherols, proteins, dietary fibers, melatonin, and folate. This study showed that *J. regia* contains a variety of chemical compounds with different biological activities (Alinia-Ahandani, 2018; Liu et al., 2021; Verma and Sharma, 2022).

Walnuts are a good source of essential fatty acids and tocopherols. Some sources reported that 17 compounds were identified in walnut leaves. 9 of them are epicatechin, syringin-o-hexoside, myristicin-3-o-glucoside, myristicin-3-o-pantoside, scoltin, taxifolin-pantoside, quercetin glucuronide, kaempferol pantoside, and kaempferol rhamnoside. Depending on various factors such as geographical location, temperature, time, a plant has a different chemical composition in different countries. Recently, different parts of the walnut tree such as leaves, bark and fruit are used in the world. Researchers have reported that the chemical composition of walnuts varies in different climates. The fruits of walnut trees are valuable and edible. And their oil is rich in polyunsaturated fatty acids, tocopherols and phytosterols (Zhao et al., 2014; Hassani et al., 2020; Sheydaei and Alinia-Ahandani, 2021).

Juglone with a molecular weight of 174.16 and a formula of $C_{10}H_5O_2$ (OH) is the most prominent substance in different organs of the walnut tree which is then converted to juglone through hydrolysis. Juglone is an alkaloid substance that is slightly soluble in hot water and moderately soluble in alcohol. As a result, it can be one of the effective ingredients in walnut leaves because other substances in walnut leaves are often water-soluble or fat-soluble. The green shell of the walnut tree fruit contains emulsion, glucose and organic substances such as citric acid, malic acid, phosphate and calcium oxalate. Juglone and phenolic compounds are the most important compounds found in the leaf and green shell of walnut (Jaimand et al., 2004).

As a toxic compound, juglone is found only in fresh and green walnuts, but it does not have such properties. The green shell of the walnut is a by-product with little use. Due to its phytochemical source, walnut shell has been shown to increase the value of walnut products. Compared to using a by-product produced in large quantities (Delaviz et al., 2017; Sheydaei et al., 2021).

We mentioned on the title of this paper as a practical look at the medical use of Iranian green walnut skin in the world, and we focused on expressing the medicinal uses of walnut. Although in various climatic conditions, we can see varieties in medicinal compounds depending on temperature, humidity and even acidity. Remarkably, some secondary metabolites like phenolic and flavonoid compounds are synthesized in different conditions. Finding these differences needs regarding relevant tests on species from various climates (Zhao et al., 2014; Jahanbani et al., 2016; Sheydaei and Alinia-Ahandani, 2020).

The purpose of this research is to investigate the medicinal effects of walnuts in different climates and the effect of the environment on the medicinal effects of species. We reviewed various researches in this field and presented their results in this report.

MATERIALS AND METHOD

In order to collect the needed materials, it was tried to use 40 related papers which were between 2000 till 2022 and sites in related journals and indexed in sources such as SID, Springer, ScienceDirect, Wiley, Taylor & Francis and etc. For this purpose, the search was done through key words such as “Walnut and Medical applications”, “*J. regia* and medical applications”, “Medical use of walnut shell” and etc. At the end, it was tried to summarize and compare the contents in a concise and useful way.

RESULTS

Recently, the use of medicinal plants has increased significantly. So that today it is necessary to use traditional medicine as well as medicinal plants with the aim of producing more effective drugs with less side effects and determining effective doses. *J. regia* is a medicinal plant with different properties, which is less considered in traditional medicine despite its great therapeutic potential. The green skin of the immature fruit of *J. regia* (Persian walnut) has a wide range of medicinal effects, which has a

long history in the treatment of malignant tumors in traditional Chinese medicine. Flavonoids are the primary constituents of *J. regia* green peel as well as the main active components. In recent years, compounds extracted from traditional Chinese medicine have attracted more attention with their antitumor activity against gastric cancer. In traditional Chinese medicine, the green skin of the unripe fruit is called Qinglongi and it is used to expel heat and toxins, expel wind and ringworm, and relieve pain and dysentery. Modern pharmacological studies have shown that the green bark of *J. regia* has a wide range of medicinal effects, including anti-inflammatory, analgesic, antibacterial, antioxidant and antitumor. Effects There are complex chemical compounds in the bark of *J. regia*, including naphthoquinones, glycosides, polysaccharides, flavonoids, diarylheptanoids, terpenoids, organic acids and tannins (Croitoru et al., 2019; Wei et al., 2022). To extract the phenolic compounds of the green peel, double solvent systems (ethanol/water) are used, which are preferable to single solvent systems, and the extracts are taken using a shaker incubator (Taheri et al., 2020). In the world market, there are so many herbs which have some medical activities and reactions and are a good source for curing minor to major issues such as colds, coughs, skin rashes, bacterial and fungal infections, diabetes, cancer, arthritis, tuberculosis, etc. Various parts of herbs such as roots, bark, fruit, flowers, seeds, leaves, stems, etc. and their secondary products such as gum, resin demonstrate biological activity which could be applied as important parts in traditional medicine (Verma and Sharma, 2020).

In traditional medicine, walnut root is used to treat diabetes, its leaves are used to treat rheumatic pains, fever, diabetes, and skin diseases. And its flowers are used to treat malaria and rheumatic pains. As far as Iranian traditional medicine is concerned, this plant is widely used in Iranian cooking to treat various diseases. Walnut leaves are used in traditional medicine to reduce blood glucose and improve diabetes. According to studies, walnut leaves contain compounds that are effective for health. And they are widely used in traditional medicine to treat venous insufficiency and hemorrhoid symptoms. In some cases, they are used as anti-diarrheal and anti-parasitic drugs, as well as blood purifiers. The results show that extensive research has been done on the medicinal effects of walnuts in the last two decades. Different parts of this plant, such as its leaves, skin and fruit, have the property of reducing blood sugar in diabetic animals (Delaviz et al., 2018).

Anti-Cancer Activity

The green skin of the immature fruit of *J. regia* (walnut) has a wide range of medicinal effects, which has a long history in the treatment of malignant tumors in traditional Chinese medicine. Flavonoids are the primary constituents of *J. regia* green peel as well as the main active components. Recent studies show the anti-cancer effects of green walnut shell. Gastric cancer is a malignant tumor of the gastrointestinal tract. This cancer has a high incidence and low survival rate and is the fifth most common cancer and the third leading cause of cancer death worldwide. The 5-year survival rate of gastric cancer patients is only 25-30%. Cyclophosphamide has been the drug of choice for the treatment of gastric cancer, but it has serious side effects. In contrast, traditional Chinese medicines with immunomodulatory function are characterized by mild side effects, good antitumor activity, and are not harmful to immune function. In this study, tumor inhibition rate in mice was 39.86, 32.87 and 22.03% respectively. Lymphocyte proliferation and macrophage phagocytosis of model mice were increased, indicating that JRF (whole green walnut skin flavonoids) can inhibit the growth of gastric cancer in mice, and this effect can be attributed to its immune regulation. The immune system is the main defense system of the body against tumor (Alinia-Ahandani et al., 2019; Wei et al., 2022).

Anticancer activity was performed on *J. regia*, which affects the survival of human breast and colon cancer cells. The 3-(4,5-dimethylthiazol-2-yl)-2,5-diphenyltetrazolium bromide (MTT) method was used to detect the viability of cancer cells. Hydrolyzed walnut protein was used against breast and colon cancer cell lines. Chymotrypsin shows good anticancer activity. Chymotrypsin hydrolyzate inhibits breast MDA-MB 231 and HT-29, a colon cancer cell line. Peptide fraction showed inhibition of cell growth by 63%±1.73% for breast cancer and 51%±1.45% for colon cancer cells (Jahanbani et al., 2016).

Anti-diabetic activity

The medical uses of walnut have been mentioned many times in the sources of Iranian traditional medicine. Walnut leaves are one of the natural medicines that are recommended to diabetic patients in traditional medicine. One of the major compounds in different parts of the walnut plant is juglone, which has been limited in research. It has been reported in a research that walnut skin extract reduces the complications of diabetes. Leaves and fleshy green fruits of walnut trees are used as blood sugar lowering agents in traditional Iranian medicine. The results of some previous studies have shown that the infusion of walnut and olive leaves has the effect of reducing blood sugar in diabetic patients. In another study, it has been proven that walnut leaf infusion was effective in reducing blood glucose levels in diabetic patients. Some researchers have also reported that the consumption of hydroalcoholic extract of walnut leaf dose-dependently reduces the blood glucose level in diabetic rats. They also believed that the effect of the hydroalcoholic extract of walnut leaves in reducing blood glucose levels was comparable to drugs such as metformin (Alinia-Ahandani et al., 2020; Wang et al., 2020).

Antioxidant activity

Antioxidant activity on different extracts of bark and green peel of *J. regia* showed that they investigated the inhibitory effect of DPPH (2,2-diphenyl-1-picrylhydrazyl) and cyclophosphamide-induced urinary toxicity in rats. With the increase in the concentration of the extract, the radical scavenging activity also increased. It was researched that all parts of walnut such as shell, leaf, seed, fruit show antioxidant activity. All the methanol extracts show higher antioxidant activity than the petroleum ether extract (Rusu et al., 2020; Werma et al., 2020). Antioxidant activity mostly is assessed by measuring thiobarbituric acid reactive substances (TBARS) and by oxidative hemolysis inhibition methods (OxHLIA). It must be said that, extract is diluted at a concentration of 10 mg/mL (distilled water and PBS solution for TBARS and OxHLIA assay, respectively), next, the subsequent dilutions (25-500 µg/mL) are carried out. The TBARS assay is done by measuring of the color intensity of malondialdehyde-thiobarbituric acid (MDA-TBA) at a wavelength of 532 nm, following the methodology (Vieira et al., 2020).

Several studies have shown the antioxidant potential of walnut products, especially fruits, leaves, and alcoholic substances produced from green fruits. In biological systems, oxidative stress is caused by an imbalance between the production of reactive oxygen species (ROS) and the antioxidant defense systems of some of the main cellular components, including lipids, proteins, and DNA (Akgül et al., 2016; Kına et al., 2021; Pehlivan et al., 2021). Excessive production of ROS or reduced antioxidant defenses may contribute to the development of several dangerous diseases. Walnuts are associated with antioxidant properties that are useful in the treatment of chronic diabetic patients. Some studies have shown that the fruits of walnut trees contain vitamin C and polyphenols with antioxidant effects (Sevindik et al., 2016; Uysal et al., 2021). According to recent research, the leaves of walnut trees have secondary metabolites that provide a strong antioxidant effect. The presence of antioxidant compounds in walnuts may lead to the collection of free radicals and their inactivation. As a result, protecting the cell membrane and various compounds of living organisms against harmful effects. Additionally, choices with moderate antioxidant activity may provide a significant marketing advantage due to consumer preference for antioxidant-rich products (Vinson and Cai, 2012; Wang et al., 2015; Sevindik et al., 2018; Alinia-Ahandani et al., 2019).

The use of natural antimicrobial compounds to produce food additives in factories is increasing due to the desire of consumers to avoid chemical preservatives and increasing resistance to antibiotics. In a way, access to plant resources is unlimited and affordable, and the ability of plants to treat all kinds of diseases has been proven from the past to the present (Sevindik et al., 2017; Zhao et al., 2018; Alinia-Ahandani et al., 2020). Some experienced methods for analyzing of antimicrobial effects are being worked. As mentioned, The hydroethanolic extract of walnut green shell would be dissolved in a mixture of dimethyl sulfoxide (DMSO) + Mueller-Hinton broth (MHB) / tryptic soy broth (TSB) (95 + 5%, v/v) to obtain a final concentration of 100. mg/ml for the stock solution. In some researches, antimicrobial potential is assessed applying five Gram-negative bacteria (*Escherichia coli*, *Proteus mirabilis*, *Klebsiella pneumoniae*, *Pseudomonas aeruginosa* and *Morganella morganii*) and three Gram-positive bacteria (*Enterococcus faecalis*, *Listeria monocytogenes-Rs A-Morganius*) (Vieira et al., 2020). In some other herbal assessment, leaves and fruits have been used in medicine. Studies have shown that walnut products, especially the shell, bark, leaves, fruit, and special compounds of juglone are associated with antimicrobial activities. Considering the economic value of the walnut fruit and the properties of its various parts, especially the oil and antioxidant compounds of the shell, we need more extensive studies in this field, especially since the properties and compounds of walnut can be different depending on different climates, as a result of the effects It can also have a different medicine that this changing feature of properties dependent on geography prompts us to advance our studies according to a more specialized climate (Ahandani et al., 2013; Fukuda and Yoshida, 2004).

DISCUSSION

Research results show. Walnut green shell (WGH) has a special place as an effective medicine in the treatment of diseases in traditional Iranian medicine. Different parts of Iranian walnut have been used to treat a wide range of diseases, including skin disorders, cancer, infectious diseases, diarrhea, blood sugar, anorexia, worm arthritis, sinusitis, eczema, asthma. Although various medicinal forms of walnut green husk (WGH), extract and burnt residue have been mentioned as wound healing agents in TIM/PM sources, previous reports indicate that this plant is a good source of phenolic compounds with high antioxidant potential. which can be used in the pharmaceutical industry. The obtained results are a step for the development of future applications using green walnut shell as well as other parts of the fruit as a source of value-added compounds with bioactive potential.

CONCLUSION

We must conclude that Persian walnut, due to its high medical and nutritional capacities, can be recognized as a main supplement in preventing cancer and also preventing cancer cells, and it should also be noted that despite the presence of many species, It requires more extensive research in the world every year.

REFERENCES

- Ahandani, E.A., Gawwad, M. R. A., Yavari, A. (2013). Extraction and preparation of psoralen from different plant part of *Psoralea corylifolia* and psoralen increasing with some elicitors. *J Plant Biol*, 2, 25-37.
- Ahandani, E.A., Ramandi, H.D., Sarmad, J., Samani, M.A., Yavari, A., Ahandani, R.A. (2014). Evaluation of morphological diversity among somepersian walnut accessions (*Juglans regia* L.) in Guilan, Northern Iran. *Int J Plant Biol Res*, 2(3), 1015.
- Akgül, H., Nur, A. D., Sevindik, M., Doğan, M. (2016). *Tricholoma terreum* ve *Coprinus micaceus*' un bazı biyolojik aktivitelerinin belirlenmesi. *Artvin Çoruh Üniversitesi Orman Fakültesi Dergisi*, 17(2), 158-162.
- Alinia-Ahandani, E. (2018a). Medicinal plants with disinfectant effects. *J Pharm Sci Res*, 10, 1-1.
- Alinia-Ahandani, E., Alizadeh-Terepoei, Z., Boghozian, A. (2019). Positive role of green tea as an anti-cancer biomedical source in Iran northern. *health-promotion*, 6(13), 15-18.
- Alinia-Ahandani, E., Alizadeh-Terepoei, Z., Sheydaei, M., Peysepar-Balalami, F. (2020). Assessment of soil on some heavy metals and its pollution in Roodsar-Iran. *Biomed J Sci & Tech Res*, 28(5), 21977-21979.
- Alinia-Ahandani, E., Fazilati, M., Boghozian, A., Alinia-Ahandani, M. (2019). Effect of ultraviolet (UV) radiation bonds on growth and chlorophyll content of *Dracocephalum moldavica* L herb. *J Biomol Res Ther*, 8(1), 1-4.
- Alinia-Ahandani, E., Nazem, H., Boghozian, A., Alizadeh, Z. (2019). Hepatitis and some effective herbs: A review. *EAS J Parasitol Infect Dis*, 1(1), 20-27.
- Alinia-Ahandani, E., Sheydaei, M., Shirani-Bidabadi, B., Alizadeh-Terepoei, Z. (2020). Some effective medicinal plants on cardiovascular diseaaes in Iran-a review. *J Glob Trends Pharm Sci*, 11(3), 8021-8033.
- Aryapak, S., Ziarati, P. (2014). Nutritive value of Persian walnut (*Juglans regia* L.) Orchards. *Am. Eurasian J. Agric. Environ. Sci*, 14, 1228-1235.
- Bahmani, M., Shirzad, H., Majlesi, M., Shahinfard, N., Rafieian-Kopaei, M. (2014). A review study on analgesic applications of Iranian medicinal plants. *Asian Pac J Trop Med*, 7, S43-S53.
- Bedia, B., Çelik, İ., Turan, A. (2019). Determination of Antioxidant Effect of Walnut (*Juglans regia* L.) on Lung and Muscle Tissue. *Doğu Fen Bil Der*, 2(1), 29-39.
- Chauhan, A., Chauhan, V. (2020). Beneficial effects of walnuts on cognition and brain health. *Nutrients*, 12(2), 550.
- Croitoru, A., Ficai, D., Craciun, L., Ficai, A., Andronescu, E. (2019). Evaluation and exploitation of bioactive compounds of walnut, *Juglans regia*. *Curr Pharm Des*, 25(2), 119-131.
- Delaviz, H., Mohammadi, J., Ghalamfarsa, G., Mohammadi, B., Farhadi, N. (2017). A review study on phytochemistry and pharmacology applications of *Juglans regia* plant. *Pharmacogn Rev*, 11(22), 145.
- Fukuda, T., Ito, H., Yoshida, T. (2004). Effect of the walnut polyphenol fraction on oxidative stress in type 2 diabetes mice. *Biofactors*, 21(1-4), 251-253.
- Habibi, A., Hamedpour-Darabi, M., Vahdati, K. (2022). Local cultural values of Persian walnut in Iran. *The Cultural Value of Trees*, 162-173.
- Hassani, D., Sarikhani, S., Dastjerdi, R., Mahmoudi, R., Soleimani, A., Vahdati, K. (2020). Situation and recent trends on cultivation and breeding of Persian walnut in Iran. *Scientia Horticulturae*, 270, 109369.
- Jafri Sayadi, M. H., Vahdati, K., Mozafari, J., Mohajer, M. R. M., Leslie, C. A. (2011). Natural Hyrcanian populations of Persian walnut (*Juglans regia* L.) in Iran. In *I International Symposium on Wild Relatives of Subtropical and Temperate Fruit and Nut Crops*, 948, 97-101.
- Jahanbani, R., Ghaffari, S. M., Salami, M., Vahdati, K., Sepehri, H., Sarvestani, N. N., Moosavi-Movahedi, A. A. (2016). Antioxidant and anticancer activities of walnut (*Juglans regia* L.) protein hydrolysates using different proteases. *Plant Foods Hum Nutr*, 71(4), 402-409.






- Jaimand, K., Baghai, P., Rezaee, M. B., Sajadipoor, S. A., Nasrabadi, M. (2004). Extraction and Identification of Juglone from Leaves and fresh peels of *Juglans regia* L. by High-Performance liquid Chromatography. *J Appl Res Med Aromat Plants*, 20(3), 323-331.
- Kına, E., Uysal, İ., Mohammed, F. S., Doğan, M., Sevindik, M. (2021). In-vitro antioxidant and oxidant properties of *Centaurea rigida*. *Turkish JAF Sci Tech*, 9(10), 1905-1907.
- Liu, M., Li, C., Cao, C., Wang, L., Li, X., Che, J., Liu, X. (2021). Walnut fruit processing equipment: academic insights and perspectives. *Food Engineering Reviews*, 13(4), 822-857.
- Pehlivan, M., Mohammed, F. S., Şabik, A. E., Kına, E., Dogan, M., Yumrutaş, Ö., Sevindik, M. (2021). Some Biological activities of ethanol extract of *Marrubium globosum*. *Turkish JAF Sci Tech*, 9(6), 1129-1132.
- Rusu, M. E., Georgiu, C., Pop, A., Mocan, A., Kiss, B., Vostinaru, O., Popa, D. S. (2020). Antioxidant effects of walnut (*Juglans regia* L.) kernel and walnut septum extract in a D-galactose-induced aging model and in naturally aged rats. *Antioxidants*, 9(5), 424.
- Sevindik, M., Akgül, H., Günal, S., Doğan, M. (2016). *Pleurotus ostreatus*' un doğal ve kültür formlarının antimikrobiyal aktiviteleri ve mineral madde içeriklerinin belirlenmesi. *J Kast Forf*, 16(1), 153-156.
- Sevindik, M., Akgul, H., Pehlivan, M., Selamoglu, Z. (2017). Determination of therapeutic potential of *Mentha longifolia* ssp. *longifolia*. *Fresen Environ Bull*, 26(7), 4757-4763.
- Sevindik, M., Akgul, H., Korkmaz, A. I., Sen, I. (2018). Antioxidant potentials of *Helvella leucomelaena* and *Sarcosphaera coronaria*. *J Bacteriol Mycol*, 6(2), 00173.
- Sheydaei, M., Alinia-Ahandani, E. (2020). Cancer and Polymeric-Carriers. *Biomed J Sci Tech Res* 31(2), 24107- 24110.
- Sheydaei, M., Alinia-Ahandani, E. (2021). Breast cancer and the role of polymer-carriers in treatment. *Biomed J Sci Technol Res*, 34(5), 27057-27061.
- Sheydaei, M., Edraki, M., Javanbakht, Sh., Alinia-Ahandani, E., Soleimani, M., Zerafatkhah, A. (2021) Poly(butylene disulfide) and poly(butylene tetrasulfide): Synthesis, cure and investigation of polymerization yield and effect of sulfur content on mechanical and thermophysical properties. *Phosphorus Sulfur Silicon Relat Elem*, 196(6), 578-584.
- Shigaeva, J., Darr, D. (2020). On the socio-economic importance of natural and planted walnut (*Juglans regia* L.) forests in the Silk Road countries: A systematic review. *For Policy Econ*, 118, 102233.
- Taheri, A., Mirghazanfari, S. M., Dadpay, M. (2020). Wound healing effects of Persian walnut (*Juglans regia* L.) green husk on the incision wound model in rats. *Eur J Transl Myol*, 30(1), 210-218.
- Uysal, İ., Mohammed, F. S., Şabik, A. E., Kına, E., Sevindik, M. (2021). Antioxidant and Oxidant status of medicinal plant *Echium italicum* collected from different regions. *Turkish JAF Sci Tech*, 9(10), 1902-1904.
- Verma, G., Sharma, V. (2020). A Scientific Update on *Juglans Regia* Linn. *Asian J Pharm Res Dev*, 8(3), 166-175.
- Vieira, V., Pereira, C., Abreu, R. M., Calhelha, R. C., Alves, M. J., Coutinho, J. A., Ferreira, O., Barros, L., Ferreira, I. C. (2020). Hydroethanolic extract of *Juglans regia* L. green husks: A source of bioactive phytochemicals. *Food Chem Toxicol*, 137, 111189.
- Vinson, J. A., Cai, Y. (2012). Nuts, especially walnuts, have both antioxidant quantity and efficacy and exhibit significant potential health benefits. *Food Funct*, 3(2), 134-140.
- Wang, J., Wu, T., Fang, L., Liu, C., Liu, X., Li, H., Min, W. (2020). Anti-diabetic effect by walnut (*Juglans mandshurica* Maxim.)-derived peptide LPLLR through inhibiting α -glucosidase and α -amylase, and alleviating insulin resistance of hepatic HepG2 cells. *J Funct Foods*, 69, 103944.
- Wang, X., Zhao, M., Su, G., Cai, M., Zhou, C., Huang, J., Lin, L. (2015). The antioxidant activities and the xanthine oxidase inhibition effects of walnut (*Juglans regia* L.) fruit, stem and leaf. *Int J Food Sci*, 50(1), 233-239.
- Wei, B., Zhu, H., Wang, K., Liu, S., Dai, Y., Liu, D., Sun, H. (2022). Antitumor and immunomodulation of total flavonoids from the green peep of *Juglans regia* L. in mouse forestomach carcinoma gastric cancer-bearing mice. *Phcog Mag*, 18(78), 328.

Zhao, H., Li, J., Zhao, J., Chen, Y., Ren, C., Chen, Y. (2018). Antioxidant effects of compound walnut oil capsule in mice aging model induced by D-galactose. *Food Nutr Res*, 62, doi: 10.29219/fnr.v62.1371

Zhao, M. H., Jiang, Z. T., Liu, T., Li, R. (2014). Flavonoids in *Juglans regia* L. leaves and evaluation of in vitro antioxidant activity via intracellular and chemical methods. *Sci World J*, doi:10.1155/2014/303878



Systematic Review of Cardiovascular Health Complications Associated with Oral Contraceptive Pills

Alamgir Khan^{*1} , Muhammad Zafar Iqbal Butt¹ , Muhammad Jamil² , Zeliha Selamoglu³ , Elifsenca Canan Alp⁴ 

^{*1}Department of Sports Sciences & Physical Education, Punjab University, Lahore, Pakistan

²Punjab Highway Patrolling Police Lahore, Pakistan

³Department of Medical Biology, Faculty of Medicine, Nigde Ömer Halisdemir University, Nigde, Turkey

⁴Department of Obstetrics and Gynecology, Faculty of Medicine, Necmettin Erbakan University, Konya, Turkey

Received : 20/11/2022

Revised : 09/12/2022

Accepted : 15/12/2022

ABSTRACT: Women using oral contraceptive pills (OCP) are consistently found to be more at risk of cardiac problems. A considerable number of women may lead to death every year due to cardiac problems caused by OCP. Besides the series of health concerns associated with OCP, the public frequently uses OCP to avoid unintended pregnancy. This study aimed to review the previous epidemiological studies to discover the facts about cardiovascular health complications associated with OCP. Analysis of previous studies reveals that acute myocardial infarction (heart attack), venous thromboembolism, and liver tumours are the major cardiovascular problems associated with OCP. The available literature shows that using OCP after eating, using of anti-inflammatory foods, performing regular exercise, low intake of sugar and maintaining quality sleep are preventive measures for reducing the side effects of OCP.

Keywords: Cardiovascular Health Complications, Medicine, Oral Contraceptive Pills.

INTRODUCTION

OCP is a form of tablet containing estrogen and progesterone hormones. These hormones are used to prevent unintended pregnancy (Gupta et al., 2008; Thomas, 2015). These hormones cause the ovulation of egg from follicles instead of changing to make up of endometrial lining in the uterus in such a way that it becomes not receptive to the ovum in the uterus and also thick the fluid in the vagina, which make the movement of sperm difficult and in this way chance of pregnancy become decreases due to the above mechanism of hormones present in the pills (Manzoor et al., 2022).

Many cardiovascular health problems, such as acute myocardial infarction (heart attack-Figure 1), venous thromboembolism and liver tumours, are associated with OCP (Sherif, 1999; Bassuk et al., 2015). The risk of cardiovascular health problems is higher in women using second-generation OCP as compared to first and second-generation (Tanis et al., 2001).

Acute myocardial infarction is myocardial necrosis and heart muscle death caused by acute coronary artery obstruction. It can be diagnosed with the help of electrocardiography (ECG) and the presence or absence of serologic markers (Sweis, 2022). The symptoms of acute myocardial infarction include chest discomfort with or without dyspnea, nausea, and/or diaphoresis. The figure below shows myocardial infarction caused by OCP

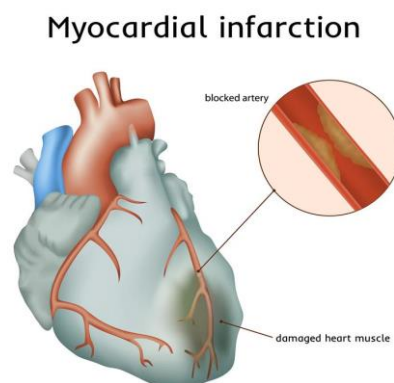


Figure 1. Myocardial infarction

Women almost the age of 35 using OCP has at high risk of myocardial infarction. The cause of myocardial infarction in oral contraceptive users is thrombotic, not atherosclerotic. In addition, alteration in lipid profile is also associated with OCP (Oliver 1970). Thrombotic is a condition where blood clots block blood vessels. It has two types. i.e. venous thrombosis and Arterial thrombosis. When the blood clots block the vein, it is called venous thrombosis; thus, when the blood clots block an artery, it is called Arterial thrombosis (Zhou et al., 2021). Both states are shown in the below Figure 2.

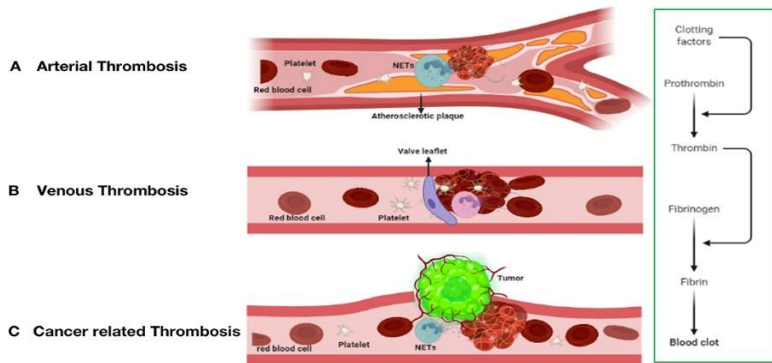


Figure 2. Thrombosis

The risk of venous thromboembolism is higher than in those not using OC (American College of Obstetricians and Gynecologists, 2012). Strategies formation for avoiding the side effects of OC is continued for a very extended period of time. Thus the association of ethinylestradiol with levonorgestrel should no longer be the only option for minimizing the risk of venous thromboembolism associated with combined OC use (Morimont et al., 2021). OC have no significant positive effect on the risk of liver cancer. The study showed that long-term use of OC can cause liver cancer as well as other health complication (An, 2015).

Excessive use of OCP increases the chances of liver tumours. Liver tumours may be of two types, i.e. adenomas and hemangiomas. The tumours made from blood vessels are known as hemangiomas cancers thus, adenomas are round-shaped tumours, usually benign (non-malignant) tumours, but infrequently can develop cancerously (Liver Doctor, 2023). The study by Hannaford et al. (1997) showed a higher risk of liver problems among women using OC containing more than 50 µg of estrogen. Nutritional supplements such as vitamin and mineral intake and, if warranted, consuming physiologic supplements of needed nutrients help reduce the side effects of OCP (Hannaford et al., 1997). Nutritional supplementations such as vitamins and minerals should be used with OCP to avoid side effects. The detail of nutrients with good sources for avoiding the side effects are given in the below table (Colorado State University, 2023).

Nutrients	Sources
Vitamin B-6	Fish, poultry, meat, whole grains, potatoes, sweet potatoes, brewer's yeast.
Folic acid	Liver, dark green leafy and stem vegetables, dried beans.
Riboflavin	Milk, meat, poultry, fish, dark green leafy vegetables, organ meats, enriched grains and cereals.
Vitamin C	Citrus fruits, juices, strawberries, cantaloupe, pineapple, broccoli, peppers, brussels sprouts, spinach, and cabbage.
Vitamin A	Green leafy vegetables (spinach, turnip tops, chard, beet greens), green stem vegetables (asparagus, broccoli), yellow vegetables (carrots, sweet potatoes, winter squash), yellow fruits (apricots, peaches, cantaloupe).
Iron	Meat, poultry, liver, fish, whole grain and enriched cereals and cereal products, dried beans and peas, prune juice, deep green leafy vegetables.
Zinc	Oysters and other seafood, meat, nuts, whole grain breads.
Copper	Oysters and other seafood, liver, nuts, dried beans and peas, dried fruits.

OCP increases inflammation in the body. Studies indicated that women with OCP have evaluated the level of C-reactive protein (CPR) as an inflammatory marker and thus it's caused pain during the monthly period, low moods, brain fog and general aches. To reduce the inflammation of OCP, it is essential to use more anti-inflammatory foods salmon, olive oil, green leafy vegetables, raw nuts, herbs & spices (Eve Wellness, 2023).

The menstrual cycle, OCP and exercise are all interrelated with each other. OCP affects the menstrual cycle similarly, the women performing exercise may be proven little to the side effects of OCP (Elliott-Sale et al., 2020). OCP causes a change in the menstrual cycle of women therefore avoiding OCP can help one to maintain her performance. In addition, regular exercise is vital for maintaining the usual monthly process of women (Elliott-Sale et al., 2020). OCP can potentially hurt blood pressure, insulin production and cardiovascular activities. Thus low-fat diet is considered essential for reducing the side effects of OCP (Straznick et al., 1998).

Women need more sleep as compared to men, and thus during the monthly cycle, women may face the problem of sleep. Similarly, sleep quality may be maintained with the help of hormonal contraception (Norelle Hentschel, 2019) Research evidence shows that quality sleep also helps reduce OCP's side effects

CONCLUSION

Epidemiological studies show that acute myocardial infarction (heart attack), venous thromboembolism, and liver tumours are the major cardiovascular problems associated with OCP. The available literature shows that using OCP after eating, using anti-inflammatory foods, performing regular exercise, eating a low sugar intake and maintaining quality sleep are preventive measures for reducing the side effects of OCP. In addition, alternative methods like a diaphragm, cervical cap, spermicides, male and female condoms and the sponge are considered a safe reference from a health point of view.

CONFLICT OF INTEREST

No conflict of interest was declared by the authors.

REFERENCES

- American College of Obstetricians and Gynecologists. (2012). Risk of venous thromboembolism among users of drospirenone-containing oral contraceptive pills. Committee Opinion No. 540. *Obstetrics Gynecol*, 120, 1239-1242.
- An, N. (2015). Oral Contraceptives Use and Liver Cancer Risk: A Dose–Response Meta-Analysis of Observational Studies. *Medicine*, 94(43), e1619.
- Bassuk, S. S., Manson, J. E. (2015). Oral contraceptives and menopausal hormone therapy: relative and attributable risks of cardiovascular disease, cancer, and other health outcomes. *Annals of epidemiology*, 25(3), 193-200.
- Colorado State University, U.S. (2023). Department of Agriculture and Colorado counties cooperating. Available <https://extension.colostate.edu/docs/foodnut/09323.pdf>. Accessed 12 March 2023
- Elliott-Sale, K. J., McNulty, K. L., Ansdell, P., Goodall, S., Hicks, K. M., Thomas, K., Swinton, P.A., Dolan, E. (2020). The effects of oral contraceptives on exercise performance in women: a systematic review and meta-analysis. *Sports medicine*, 50(10), 1785-1812.
- Eve Wellness. (2023). Available <https://engage.evewellness.com/blog/on-the-pill-here-are-5-ways-to-support-your-body> Accessed 12 March 2023
- Gupta, N., Corrado, S., Goldstein, M., & Gupta, C. (2008). Hormonal contraception for the adolescent. *Pediatr Rev*, 29(11), 386-96.
- Hannaford, P. C., Kay, C. R., Vessey, M. P., Painter, R., & Mant, J. (1997). Combined oral contraceptives and liver disease. *Contraception*, 55(3), 145-151.
- Liver Doctor. Available <https://www.liverdoctor.com/the-oral-contraceptive-pill-may-be-putting-your-liver-at-risk/> Accessed 12 March 2023

- Khan, M., Khan, A., Butt, M. Z. I., Khan, S., Jamil, M., Ozdemir, B., Alp, E.C., Selamoglu, Z. (2022). Oxidative Stress and Menstrual Complications Caused by Vaccination of COVID-19 Among Females Athletes. *Cumhuriyet Medical Journal*, 44(1), 38-43.
- Morimont, L., Haguët, H., Dogné, J. M., Gaspard, U., Douxfils, J. (2021). Combined oral contraceptives and venous thromboembolism: review and perspective to mitigate the risk. *Frontiers in endocrinology*, 12, 769187
- Norelle Hentschel. (2019). Available <https://medium.com/@norelle.hentschel/6-ways-the-oral-contraceptive-pill-disrupts-sleep-82e5c66dcd4a> Accessed 12 March 2023
- Oliver, M. F. (1970). Oral contraceptives and myocardial infarction. *Br Med J*, 2(5703), 210-213.
- Sherif, K. (1999). Benefits and risks of oral contraceptives. *American journal of obstetrics and gynecology*, 180(6), S343-S348.
- Straznicky, N. E., Barrington, V. E., Branley, P., Louis, W. J. (1998). A study of the interactive effects of oral contraceptive use and dietary fat intake on blood pressure, cardiovascular reactivity and glucose tolerance in normotensive women. *Journal of hypertension*, 16(3), 357-368.
- Sweis, R.N. (2022). Acute myocardial infarction (MI). Northwestern University Feinberg School of Medicine.
- Tanis, B. C., Van Den Bosch, M. A., Kemmeren, J. M., Cats, V. M., Helmerhorst, F. M., Algra, A., Graf, Y.V., Rosendaal, F. R. (2001). Oral contraceptives and the risk of myocardial infarction. *New England Journal of Medicine*, 345(25), 1787-1793.
- Thomas, S. V. (2015). Controversies in contraception for women with epilepsy. *Annals of Indian Academy of Neurology*, 18(3), 278.
- Zhou, Y., Tao, W., Shen, F., Du, W., Xu, Z., Liu, Z. (2021). The emerging role of neutrophil extracellular traps in arterial, venous and cancer-associated thrombosis. *Frontiers in Cardiovascular Medicine*, 8, 786387.



Application of Experimental Design Methodology to Optimize Azithromycin Removal by Graphene/Iron Oxide Nanocomposite

Saeed Ullah Jan^{*1}, Saad Melhi², Nadia Bibi³, Anam Nisar³, Sana Faryal³, Nabeela³, Tahira Naz³, Amina Bibi³, Aman Ullah³, Zeliha Selamoglu⁴

^{*1}Department of Chemistry, Chakdara Lower Dir, University of Malakand, Pakistan

²Department of Chemistry, College of Science, University of Bisha, Bisha, Saudi Arabia

³Department of Chemistry, GPGC Timergara Lower Dir, Pakistan

⁴Department of Medical Biology, Faculty of Medicine, Nigde Omer Halisdemir University, Nigde, Türkiye

Received : 15/11/2022

Revised : 26/12/2022

Accepted : 29/03/2023

ABSTRACT: Currently, the occurrence and fate of antibiotics in the aquatic environment has become a very serious problem in that they can potentially and irreversibly damage the ecosystem and human health. For this reason, interest has increased in developing strategies to remove antibiotics from water. In this study, we report the several adsorption parameters including the adsorbent dosage, the initial azithromycin concentration, contact time, temperature, and pH were studied. The maximum adsorption Q_{max} (9.89 mg g⁻¹) was obtained after shaking the mixture for 30 min, at 298 K, and at neutral pH. The adsorption isotherm was analyzed by different isotherm models. The Langmuir and Freundlich isotherm models were found fitted to data well. The adsorption process follows second-order pseudo kinetics. The adsorption was endothermic ($\Delta H^\circ = 39.64$ kJ/mol), effective ($\Delta S^\circ = 174$ kJ/mol·K) and spontaneous ($\Delta G^\circ = -15$ KJ/mol). Overall, the findings in this study confirm that Graphene/Fe₂O₃ is a feasible and viable option for removing azithromycin from water in terms of water quality improvement and urgent antibiotics pollution control.

Keywords: Azithromycin dihydrate, Graphene/Fe₂O₃ nanocomposite, Kinetics, Thermodynamics parameters

INTRODUCTION

The presence of pharmaceutical and personal care products (PPCPs) in the receiving water has been reported to be an emerging and persistent risk for living beings. Emerging pollutants includes pharmaceuticals, pesticides, personal care products, hormones, detergent and food additives etc. (Abidi et al., 2019; Balarak et al., 2021a). Among PPCPs, β -lactam antibiotics such as Azithromycin (AZM) have been widely used to prevent the growth of bacteria by synthesizing their cell walls. These antibiotics, due to insufficient metabolism in the human body are excreted in significant amounts and enter the wastewater treatment plant. Antibiotics are a class of pharmaceuticals used against bacteria and other microbes (Cheng et al., 2020). They are classified into Penicillin, Cephalosporin, Aminoglycosides, Macrolides, Tetracycline and Fluoroquinolones (Abidi et al., 2020). They are extensively used and not fully metabolized and excreted through feces and urine. They are also continuously discharged to environment from hospitals and pharmaceutical industries and cause health problems like endocrine disrupting effects in aquatic organisms and produces antibiotics resistance in pathogens (Al-Mamun et al., 2019). Therefore, the rem Balarak et al. (2021b), report the adsorptive removal of azithromycin (AZM) antibiotics using activated porous carbon prepared from *Azolla filiculoides* (AF) (AFAC). The influence of the adsorption process variables, such as temperature, pH, time, and adsorbent dosage, is investigated and described. Rostamian and Behnejad (2016), study the adsorption properties of sulfamethoxazole (SMX) as an antibiotic were promoted by graphene nanosheet (GNS) and Graphene oxide nanosheet (GOS). The five factors influencing the adsorption of SMX (initial SMX concentration, initial solution pH, amount of adsorbent, temperature and contact time) were studied. Ehtesabi et al. (2019), study, a one-step hydrothermal reduction method applied for the preparation of 3D porous graphene hydrogel adsorbents. The characteristic properties of synthesized graphene hydrogels were obtained using scanning electron microscopy, Raman spectroscopy, Fourier transform infrared spectroscopy and Brunauer-Emmett Teller. Wahab et al. (2021), prepared, activated carbon (AC) and magnetic activated carbon (MAC) from *Dalbergia sissoo* sawdust for the removal of antibiotic Azithromycin (AZM) from aqueous solution. The effect of initial concentration, contact time, pH, adsorbent dosage, and the temperature were investigated for both the adsorbents. Cuerda-Correa et al. (2019), study the application of advanced oxidation processes (AOPs) for the removal of antibiotics from water has been reviewed. The present concern about water has been exposed, and the main problems derived from the presence of emerging pollutants have been analyzed. Photolysis processes, ozone-based AOPs including ozonation, O₃/UV, O₃/H₂O₂, and O₃/H₂O₂/UV, hydrogen peroxide-based methods (i.e., H₂O₂/UV, Fenton, Fenton-like, hetero-Fenton, and photo-Fenton), heterogeneous photo catalysis (TiO₂/UV and TiO₂/H₂O₂/UV systems), and sonochemical and electro oxidative AOPs have been reviewed. The main challenges and prospects of AOPs, as well as some recommendations for the improvement of AOPs aimed at the removal of antibiotics from

wastewaters, are pointed out. Talaiekhosani et al. (2020), study the removal of azithromycin from water using ultraviolet radiation (UV), Fe (VI) oxidation process and ZnO nanoparticles. The effect of different parameters such as pH, temperature, hydraulic retention time (HRT), the concentration of Fe (VI) and ZnO nanoparticles and UV intensity on the removal of azithromycin from water was investigated. The optimal conditions for the removal of azithromycin were a pH of 2. Carabineiro et al. (2011), determined the adsorption capacity of ciprofloxacin (CPX) on three types of carbon-based materials: activated carbon (commercial sample), carbon nanotubes (commercial multi-walled carbon nanotubes) and carbon xerogel (prepared by the resorcinol/formaldehyde approach at pH 6.0).

Different techniques have been used for the removal of antibiotics from water. They include membrane filtration, electrochemical methods, degradation, adsorption method, ion exchange, solvent extraction and reverse osmosis etc (Behnajady et al., 2006; Bian et al., 2019). Adsorption is an efficient technique due to its cost effectiveness, simple in operation and no production of secondary pollution (Çağlar Yılmaz et al., 2020). Various adsorbents such as graphene, carbon nanotubes, activated carbon, Metal-Organic Frameworks (MOF) and chitosan have been used to remove antibiotics from water (Deng et al., 2015).

The researchers are trying to explore an efficient, nontoxic, selective and cost-effective adsorbent for the removal of antibiotics from water.

The composite of graphene/Fe₂O₃ is a good adsorbent with the specific characteristics for the elimination of antibiotics from water. The structure of graphene is two dimensional in which carbon atoms has sp² hybridization packed in a hexagonal lattice like honey comb. It has high adsorption capacity due to its large surface area (Çalışkan Salihi et al., 2021). The presence of Fe₂O₃ nanoparticles on the surface of graphene can avoid the agglomeration of graphene sheets and maintain its high surface area. Graphene/ Fe₂O₃ composite can be prepared by various methods like sol-gel method, hydrothermal method and microwaves method (Xu et al., 2013; Lyubutin et al., 2018).

METHODS AND RESULTS

Chemicals and Reagents

The chemicals such as Ethanol (C₂H₅OH), Iron oxide (Fe₂O₃), sodium hydroxide (NaOH), graphene and hydrochloric acid (HCl) manufactured by Sigma Aldrich were used in this study without any pretreatment.

Apparatus/Instruments

In this study Sonicater (power sonic 405), pH meter (pH7110), Electronic Balance (Shimadzu X200), wrist Action Shaker (Model 75), hot plate (MSH 20A), Water bath, UV-Vis spectrophotometer (UVD-2960 Labomed. Inc.), etc. were used.

Adsorbent

The adsorbent Graphene/Iron oxide composite was prepared by solvothermal method. In this method 0.33 mg/mL of Fe₂O₃ dispersed in 300 mL ethanol. The solution was sonicated for 40 minutes in power sonic 405. Similarly, 2.5 mg/mL of graphene were dispersed in ethanol. Then after sonication 300 mL of Fe₂O₃ solution was added carefully drop by drop to the 200 mL dispersion solution of graphene. The prepared mixture was then placed in water bath to evaporate the ethanol. After that the solid mass of graphene/Iron oxide composite obtained. It was dried at 70 °C temperature in oven for four hours.

Adsorbate

The adsorbent was used for the adsorption of Azithromycin antibiotic in this study. Azithromycin dihydrate is a white crystalline powder with a molecular formula of C₃₈H₇₂N₂O₁₂·2H₂O and a molecular weight of 785.0. Figure (1).

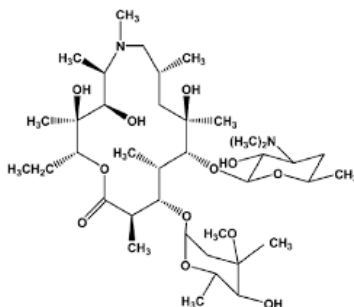


Figure 1. Chemical structure of Azithromycin dihydrate

The pH had the highest effect on Azithromycin removal

Procedure

Preparation of Stock Solution of Adsorbate

In this study, 1000 ppm stock solution of adsorbate was prepared by dissolving 0.5 g of different Azithromycin dihydrate in distilled water in a 500 mL volumetric flask. The flask was filled up to the mark by adding more water. The stock solution was stored and diluted by dilution formula ($C_1V_1 = C_2V_2$) to the required concentrations when required.

Investigation of maximum absorbance (λ_{max})

To investigate the maximum absorbance wavelength (λ_{max}) of adsorbate various concentration of Azithromycin dihydrate were examined in UV-Visible range (200-800 nm) by using UV-Visible spectrophotometer (UVD-2960 Labomed. Inc). The maximum absorbance wavelength (λ_{max}) measured for Azithromycin dihydrate was 236 nm. These values of λ_{max} of Azithromycin dihydrate was used in the rest of experimental adsorption studies (Ibrahim et al., 2017).

Working or Calibration curve

The calibration curve for Azithromycin dihydrate was determined by plotting different concentration solution of Azithromycin dihydrate versus absorbance. The absorbance was investigated by using UV-Visible spectrophotometer. The calibration curve for the Azithromycin dihydrate is shown in the Figures 2.

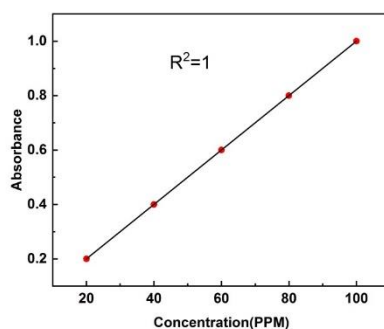


Figure 2. Calibration Curve of Adsorption of Azithromycin onto Graphene/Fe₂O₃ nanocomposite

Preparation of different pH solutions

The different pH solutions ranges from pH 1 to pH 7 were prepared in this study. The pH of solutions was adjusted by using 0.1 M hydrochloric acid (HCl) and 0.1 M sodium hydroxide (NaOH) solutions. The pH of solution was determined and adjusted by using pH paper and pH meter. Distilled water having pH 7 was considered as neutral solution.

By plotting absorbance versus concentration of antibiotics a linear regression equation was obtained from which the antibiotics concentration in the solution was calculated. The percent adsorption and equilibrium adsorption of antibiotics was calculated by applying the following equations.

$$\% \text{ Removal} = \left(\frac{C_0 - C_e}{C_0} \right) \times 100 \quad (1)$$

$$Q_e = C_0 - C_e \times \frac{V}{m} \quad (2)$$

Where, Q_e is the equilibrium concentration of adsorbate (antibiotics) (mg/g), C_0 is the initial concentration (mg/L), C_e represents the final concentration and V show the volume of solution in (L) and m is mass of adsorbent in (g) respectively.

Batch Mode Adsorption study

In this research work the adsorption of antibiotic Azithromycin Dihydrate on graphene/Iron oxide composite was investigated by batch mode adsorption process. The conditions which affect the adsorption process such as pH, adsorbent dose, contact time,

The pH had the highest effect on Azithromycin removal

concentration of antibiotics and temperature were investigated. To understand the mechanism of adsorption, various kinetic equations and isotherm models were applied. Thermodynamics parameters were also calculated from experimental data.

Influence of pH on adsorption of antibiotics

Adsorption process is very sensitive to the pH of medium. The pH of medium could change the surface charge of both adsorbate and adsorbent which affect the electrostatic force of attraction between them (Kadirvelu et al., 2005). The influence of pH on adsorption of antibiotic was studied at pH range from (1-7). The initial concentration of antibiotics was 50 ppm, adsorbent weight 0.005 g and shaking time 60 minutes. The maximum adsorption of Azithromycin dihydrate was at pH 7. The results are given in Figure 3. The graphene/Iron oxide nanocomposite used for removal of antibiotics contained different surface functional groups that show variable behavior by changing pH of the solution. The maximum adsorption of Azithromycin dihydrate was investigated at pH 6-7. The surface of Azithromycin dihydrate positive charge at pH < 3.0 and electrostatic repulsion decreases adsorption (Nigam et al., 2000). When pH increases from 3 to 6 the surface of Azithromycin dihydrate become negative charge can easily bind with positive charge adsorbent. At pH 7 the Azithromycin dihydrate exists in zwitterion and show maximum adsorption.

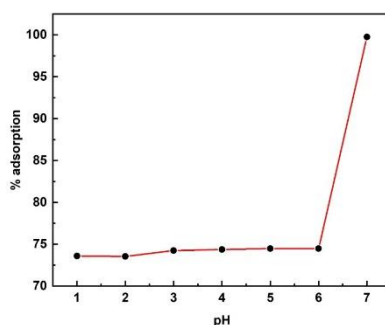


Figure 3. The pH effect on adsorption of Azithromycin dihydrate by graphene/Iron oxide nanocomposite

Effect of antibiotic concentration on adsorption

To explore the effect of initial concentration of the antibiotic adsorption on graphene/Fe₂O₃ composite were studied in range from (20 ppm to 160 ppm). The experiment was performed under optimized conditions. From the experimental results it was investigated that the adsorption efficiency of adsorbent increase with increase in concentration of antibiotics as shown in Figure 4. The increase in percent adsorption with increase in concentration of antibiotic was due to the available active sites on the surface of graphene/Fe₂O₃ composite (adsorbent).

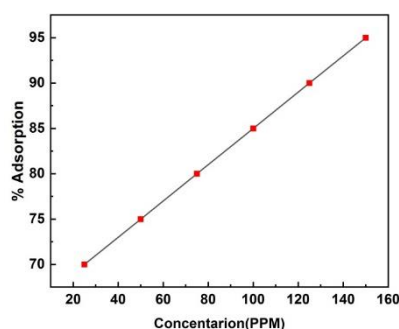


Figure 4. The Concentration effect on adsorption of Azithromycin dihydrate by graphene/Iron oxide nanocomposite

Various adsorption isotherms were applied to experimental data to understand the mechanism of adsorption. Freundlich model was used in the liner form as given bellow.

$$\log q_e = \log K_F + 1/n \log C_e \quad (3)$$

Where q_e is amount of adsorbate (antibiotics) adsorbed at equilibrium, C_e represents adsorbate concentration at equilibrium. K_F and $1/n$ are Freundlich constants which show adsorption efficiency and adsorption intensity respectively. The values of K_F and

The pH had the highest effect on Azithromycin removal

1/n were calculated from slop and intercept by plotting qe versus Ce. The experimental results obtained from Freundlich adsorption isotherm (Figure 5). This indicates that adsorption data agreed well with Freundlich isotherm model (Ng et al., 2002; Majd et al., 2021). The values of Freundlich isotherm constants K_F and 1/n for Azithromycin dihydrate is given in Tables 1.

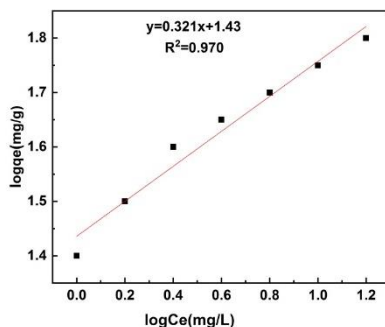


Figure 5. Freundlich adsorption isotherms for azithromycin Dihydrate adsorption onto graphene/Fe2O3 nanocomposite

The experimental data was subjected to Langmuir isotherm model (Langmuir et al., 1918). According to this model the adsorption of adsorbate occur at specific homogeneous active sites on surface of adsorbate. The following linear form of Langmuir equation was applied to experimental data.

$$\frac{C_e}{q_e} = \frac{1}{Q_{max}} C_e + \frac{1}{K_L Q_{max}} \quad (4)$$

Here, Q_{max} represents maximum adsorption capacity, q_e represent the amount of adsorbate adsorbed on adsorbent, C_e show equilibrium concentration of adsorbate in solution and K_L is Langmuir equilibrium constant (Ahmadi et al., 2013). The values of Q_{max} and K_L were determined from slop in the form of graphs. The values of Langmuir constants K_L and Q_{max} are given in Table 1. The value of dimensionless constant R_L of Langmuir isotherm was calculated by equation below.

$$R_L = \frac{1}{1 + K_L C_i} \quad (5)$$

Where C_i represents initial concentration of adsorbate (mg/g) and K_L is Langmuir constant

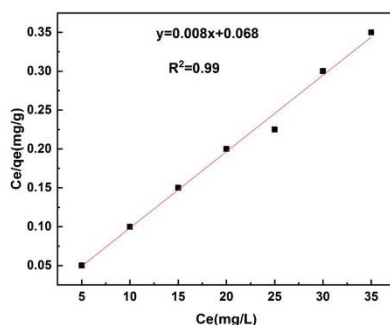


Figure 6. Langmuir adsorption isotherms for azithromycin Dihydrate adsorption onto graphene/Fe2O3 nanocomposite

Table 1. The isotherm parameters of Azithromycin Dihydrate adsorption onto graphene/Fe2O3 nanocomposite

Models	Parameters	Values
Freundlich	K_F (mg/g)	21.23978
	1/n	0.32143
	R^2	0.970
	Q_{max} (mg/g)	9.891197
	R_L (dm ³ /mol)	6.03
Langmuir	K_L (mg/g)	1.20
	R^2	0.99

Effect of the amount of adsorbent

Adsorption capacity of adsorbent is highly affected by changing the amount of adsorbent. The effect of the amount of adsorbent (graphene/Fe₂O₃) on the adsorption of antibiotics were studied at optimized pH and contact time in ranges from 0.001 to 0.015 g/10mL for azithromycin Dihydrate. The experimental results reveal that adsorption of antibiotic increases with increase in amount of adsorbent as shown in Figure 7. This is due to more availability of surface site of adsorbent for the attachment of adsorbate molecules (Hu et al., 2019). The optimum adsorption 98.71% for azithromycin Dihydrate was observed at 0.006 g of adsorbent.

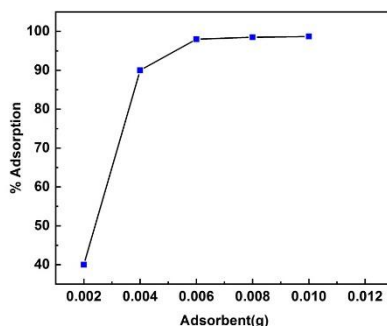


Figure 7. Influence of adsorbent does on adsorption of Azithromycin Dihydrate by graphene /Fe₂O₃ nanocomposite

Effect of shaking time

Shaking time has great effect the on adsorption process of antibiotic. The effect of shaking on adsorption of antibiotic by graphene /Iron oxide composite was investigated. The experiment was performed at shaking time from 10 to 60 minutes, adsorbent does (0.006 g), concentration of antibiotics 50 ppm, at optimum pH and room temperature. The adsorption of antibiotic was initially increased with increase in time. This because of the availability of more active sites on the surface of adsorbent at the beginning and then gradually saturation occurred. After equilibrium time no further increase in adsorption was observed (Mondal et al., 2007). The equilibrium time investigated for Azithromycin Dihydrate was 30 minutes. The experimental results are given in Figures 8, and this equilibrium shaking time was used for all experiments.

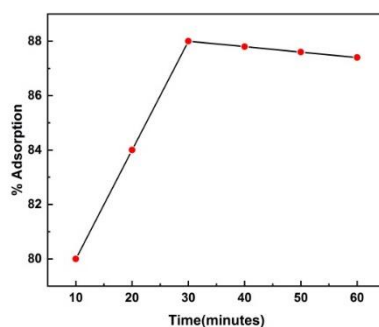


Figure 8. Effect of shaking time on adsorption of Azithromycin Dihydrate by graphene /Fe₂O₃ nanocomposite

Kinetic models were applied to understand the adsorption mechanism and rate of reaction.

The linear form of pseudo 2nd order equation was applied to experimental data as given bellow

$$t/q_t = t/q_e + 1/k_2 q_e^2 \quad (6)$$

Where q_e^2 is concentration of antibiotics adsorbed at equilibrium, q_t concentration of antibiotics at time 't' and k_2 is rate constant for pseudo 2nd order equation. The graphs t/q_t versus t were obtained with correlation coefficient R^2 values (0.999) for Azithromycin Dihydrate. The graphs are shown in the Figure 9, which reveals that the experimental data agreed well with pseudo 2nd order kinetic model (Liu, 2008; Guo and Wang, 2019)

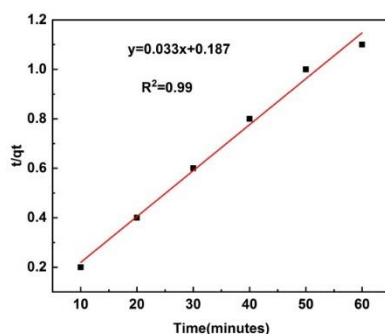


Figure 9. Pseudo 2nd order kinetic model for Azithromycin Dihydrate onto graphene / Iron oxide nanocomposite

To understand further the mechanism of adsorption Reichenberg equation was applied to experimental data. The Reichenberg (1953), equation explain that either intraparticle or film diffusion process is involved in the adsorption mechanism. The equation is given bellow

$$Q = \left(1 - \frac{6}{\pi^2}\right) e^{-Bt} \tag{7}$$

Where $Q = qt/q_e$ and Bt is a mathematical function of ‘ Q ’ which can be calculated from the following equation.

$$Bt = -0.4977 - \ln(1 - Q) \tag{8}$$

The graphs obtained from the plot of ‘ Bt ’ versus ‘ t ’ are shown in Figures 10. The linear line does not pass through origin which shows that initially intraparticle diffusion followed by film diffusion occurs between adsorbate (antibiotic) and adsorbent. The data are tabulated in Table 2.

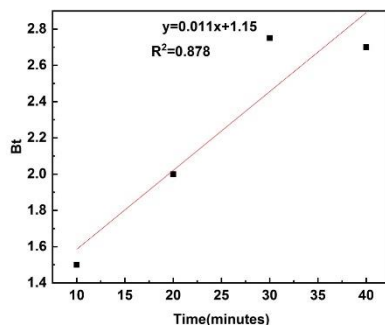


Figure 10. Reichenberg model for Azithromycin Dihydrate onto graphene/Iron oxide nanocomposite

Table 2. Different kinetic parameters of adsorption of Azithromycin Dihydrate adsorption onto graphene/Fe2O3 nanocomposite

Azithromycin Dihydrate		
Models	Kinetic parameters	Values
Pseudo second order	K_2 (g/mg ¹ min ⁻¹)	86475.47
	R^2	0.99
Reichenberg	R^2	0.878

Effect of temperature on the adsorption of antibiotic onto graphene/Fe2O3 Nano composite

Adsorption process is highly affected by change in temperature. The influence of temperature on adsorption of antibiotic Azithromycin Dihydrate was studied in the temperature range (298K to 318 K) at optimized conditions (Aksu et al., 2008). The experimental results indicate that adsorption of antibiotic on graphene/Fe₂O₃ composite decreases with increase in temperature as given in the Figure 11, show that adsorption process was exothermic in nature (Striolo et al., 2005).

The pH had the highest effect on Azithromycin removal

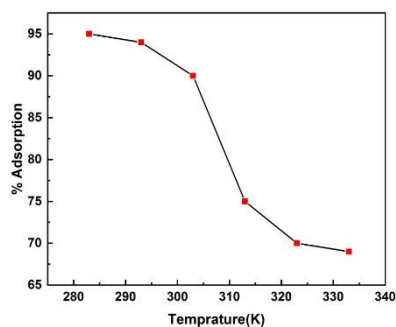


Figure 11. Effect of temperature on adsorption of onto graphene/Fe₂O₃ nanocomposite

Thermodynamic study

The different thermodynamic variables like enthalpy, entropy and Gibbs free energy were calculated with the help of the following equation.

$$\ln K_L = \frac{\Delta S}{R} - \frac{\Delta H}{RT} \quad (9)$$

$$\Delta G = \Delta H - T\Delta S \quad (10)$$

$$\Delta G = -RT \ln K_L \quad (11)$$

Where ΔS represent entropy (J/mol K), ΔH is enthalpy (kJ/mol) and ΔG is Gibbs free energy (kJ/mol), T show absolute temperature and R is gas constant (Motomura, 1978).

The value of K_L can be determined by the following equation

$$K_L = \frac{F}{1-F} \quad (12)$$

The value of F show the fraction adsorbed at equilibrium. The values of ΔS and ΔH were calculated from the slop by plotting the value of $\ln K_L$ versus $1/T$ and the results are given in Figure 12. The experimental results reveal that adsorption process was spontaneous, feasible and exothermic in nature (Pan et al., 2016). The thermodynamic parameters are given in Table 3.

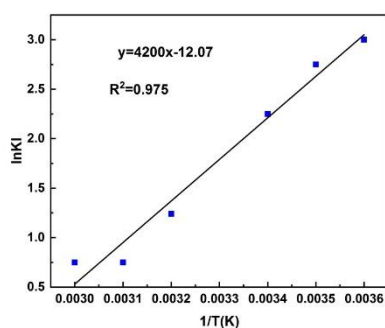


Figure 12. Change in adsorption equilibrium of Azithromycin Dihydrate onto graphene/Fe₂O₃ nanocomposite with temperature.

Table 3. The thermodynamic parameters for the adsorption of Azithromycin Dihydrate onto Graphene/Iron Oxide nanocomposite

Temperature	ΔS° kJ/mol·K	ΔH° kJ/mol·	ΔG° kJ/mol·
298	174.55	39.64	-12.39
308	174.55	39.64	-14.112
318	174.55	39.64	-15.857

CONCLUSIONS

The excessive use of antibiotics produces water pollution which leads to different environmental problems. Graphene/Fe₂O₃ composite was synthesized for the removal of antibiotics from water. The composite was used for the removal of Azithromycin dihydrate from aqueous solution. Various adsorption conditions which influence adsorption capacity of antibiotic on Graphene/Fe₂O₃ composite were optimized. The maximum adsorption capacity of Azithromycin dihydrate (98 %) at pH 7. To study the mechanism of adsorption different isotherm model and kinetic equations were applied to the adsorption data. Pseudo second order kinetic model agreed well with experimental results. The adsorption of Azithromycin dihydrate on adsorbent is fitted well to Freundlich and Langmuir models. The effect of temperature on the adsorption of antibiotic Graphene/Fe₂O₃ composite was studied and thermodynamic parameters such as ΔG , ΔS and ΔH were calculated. The results show that adsorption process is feasible, spontaneous and endothermic in nature.

CONFLICT OF INTEREST

No conflict of interest was declared by the authors.

REFERENCES

- Abidi, M., Assadi, A. A., Bouzaza, A., Hajjaji, A., Bessais, B., Rtimi, S. (2019). Photocatalytic indoor/outdoor air treatment and bacterial inactivation on Cu_xO/TiO₂ prepared by HiPIMS on polyester cloth under low intensity visible light. *Applied Catalysis B: Environmental*, 259, 118074.
- Abidi, M., Hajjaji, A., Bouzaza, A., Trablesi, K., Makhlouf, H., Rtimi, S., Assadi, A., Bessais, B. (2020). Simultaneous removal of bacteria and volatile organic compounds on Cu₂O-NPs decorated TiO₂ nanotubes: competition effect and kinetic studies. *Journal of Photochemistry and Photobiology A: Chemistry*, 400, 112722.
- Ahmadi, M. A., Shadizadeh, S. R. (2013). Induced effect of adding nano silica on adsorption of a natural surfactant onto sandstone rock: experimental and theoretical study. *Journal of Petroleum Science and Engineering*, 112, 239-247.
- Aksu, Z., Tatlı, A. İ., Tunç, Ö. (2008). A comparative adsorption/biosorption study of Acid Blue 161: Effect of temperature on equilibrium and kinetic parameters. *Chemical Engineering Journal*, 142(1), 23-39.
- Al-Mamun, M. R., Kader, S., Islam, M. S., Khan, M. Z. H. (2019). Photocatalytic activity improvement and application of UV-TiO₂ photocatalysis in textile wastewater treatment: A review. *Journal of Environmental Chemical Engineering*, 7(5), 103248.
- Balarak, D., Mahvi, A. H., Shahbaksh, S., Wahab, M. A., Abdala, A. (2021b). Adsorptive removal of azithromycin antibiotic from aqueous solution by azolla filiculoides-based activated porous carbon. *Nanomaterials*, 11(12), 3281.
- Balarak, D., Mengelizadeh, N., Rajiv, P., Chandrika, K. (2021a). Photocatalytic degradation of amoxicillin from aqueous solutions by titanium dioxide nanoparticles loaded on graphene oxide. *Environmental Science and Pollution Research*, 28(36), 49743-49754.
- Behnajady, M. A., Modirshahla, N., Hamzavi, R. (2006). Kinetic study on photocatalytic degradation of CI Acid Yellow 23 by ZnO photocatalyst. *Journal of hazardous materials*, 133(1-3), 226-232.
- Bian, X., Xia, Y., Zhan, T., Wang, L., Zhou, W., Dai, Q., Chen, J. (2019). Electrochemical removal of amoxicillin using a Cu doped PbO₂ electrode: electrode characterization, operational parameters optimization and degradation mechanism. *Chemosphere*, 233, 762-770.

- Carabineiro, S. A. C., Thavorn-Amornsri, T., Pereira, M. F. R., Figueiredo, J. L. (2011). Adsorption of ciprofloxacin on surface-modified carbon materials. *Water research*, 45(15), 4583-4591.
- Cheng, D., Ngo, H. H., Guo, W., Chang, S. W., Nguyen, D. D., Liu, Y., Wei, Q., Wei, D. (2020). A critical review on antibiotics and hormones in swine wastewater: Water pollution problems and control approaches. *Journal of hazardous materials*, 387, 121682.
- Cuerda-Correa, E. M., Alexandre-Franco, M. F., Fernández-González, C. (2019). Advanced oxidation processes for the removal of antibiotics from water. An overview. *Water*, 12(1), 102.
- Çağlar Yılmaz, H., Akgeyik, E., Bougarrani, S., El Azzouzi, M., Erdemoğlu, S. (2020). Photocatalytic degradation of amoxicillin using Co-doped TiO₂ synthesized by reflux method and monitoring of degradation products by LC–MS/MS. *Journal of Dispersion Science and Technology*, 41(3), 414-425.
- Çalışkan Salihi, E., Wang, J., Kabacaoğlu, G., Kırkulak, S., Šiller, L. (2021). Graphene oxide as a new generation adsorbent for the removal of antibiotics from waters. *Separation Science and Technology*, 56(3), 453-461.
- Deng, Y., Zhao, R. (2015). Advanced oxidation processes (AOPs) in wastewater treatment. *Current Pollution Reports*, 1, 167-176.
- Ehtesabi, H., Bagheri, Z., Yaghoubi-Avini, M. (2019). Application of three-dimensional graphene hydrogels for removal of ofloxacin from aqueous solutions. *Environmental nanotechnology, monitoring & management*, 12, 100274.
- Guo, X., Wang, J. (2019). A general kinetic model for adsorption: theoretical analysis and modeling. *Journal of Molecular Liquids*, 288, 111100.
- Hu, T., Li, Y., Gao, W., Wang, X., Tian, Y. (2019). Engineering of rich nitrogen-doped and magnetic mesoporous carbon nanospheres with predictable size uniformity for acid dye molecules adsorption. *Microporous and Mesoporous Materials*, 279, 234-244.
- Ibrahim, F. A., Wahba, M. E. K., Galal, G. M. (2017). Two spectrophotometric methods for the determination of azithromycin and roxithromycin in pharmaceutical preparations. *European Journal of Chemistry*, 8(3), 203-210.
- Kadirvelu, K., Karthika, C., Vennilamani, N., Pattabhi, S. (2005). Activated carbon from industrial solid waste as an adsorbent for the removal of Rhodamine-B from aqueous solution: Kinetic and equilibrium studies. *Chemosphere*, 60(8), 1009-1017.
- Langmuir, I. (1918). The adsorption of gases on plane surfaces of glass, mica and platinum. *Journal of the American Chemical society*, 40(9), 1361-1403.
- Liu, Y. (2008). New insights into pseudo-second-order kinetic equation for adsorption. *Colloids and surfaces A: physicochemical and engineering aspects*, 320(1-3), 275-278.
- Lyubutin, I. S., Baskakov, A. O., Starchikov, S. S., Shih, K. Y., Lin, C. R., Tseng, Y. T., Yang, S.S., Han, Z.Y., Ogarkova, Y. L., Nikolaichik, V., Avilov, A. S. (2018). Synthesis and characterization of graphene modified by iron oxide nanoparticles. *Materials Chemistry and Physics*, 219, 411-420.
- Majd, M. M., Kordzadeh-Kermani, V., Ghalandari, V., Askari, A., Sillanpää, M. (2022). Adsorption isotherm models: A comprehensive and systematic review (2010– 2020). *Science of The Total Environment*, 812, 151334.
- Mondal, P., Balomajumder, C., Mohanty, B. (2007). A laboratory study for the treatment of arsenic, iron, and manganese bearing ground water using Fe³⁺ impregnated activated carbon: effects of shaking time, pH and temperature. *Journal of hazardous materials*, 144(1-2), 420-426.
- Motomura, K. (1978). Thermodynamic studies on adsorption at interfaces. I. General formulation. *Journal of Colloid and Interface Science*, 64(2), 348-355.
- Ng, C., Losso, J. N., Marshall, W. E., Rao, R. M. (2002). Freundlich adsorption isotherms of agricultural by-product-based powdered activated carbons in a geosmin–water system. *Bioresource technology*, 85(2), 131-135.

- Nigam, P., Armour, G., Banat, I. M., Singh, D., Marchant, R. (2000). Physical removal of textile dyes from effluents and solid-state fermentation of dye-adsorbed agricultural residues. *Bioresource technology*, 72(3), 219-226.
- Pan, A., Kar, T., Rakshit, A. K., Moulik, S. P. (2016). Enthalpy–entropy compensation (EEC) effect: decisive role of free energy. *The Journal of Physical Chemistry B*, 120(40), 10531-10539.
- Reichenberg, D. (1953). Properties of ion-exchange resins in relation to their structure. III. Kinetics of exchange. *Journal of the American Chemical Society*, 75(3), 589-597.
- Rostamian, R., Behnejad, H. (2016). A comparative adsorption study of sulfamethoxazole onto graphene and graphene oxide nanosheets through equilibrium, kinetic and thermodynamic modeling. *Process Safety and Environmental Protection*, 102, 20-29.
- Striolo, A., Gubbins, K. E., Gruskiewicz, M. S., Cole, D. R., Simonson, J. M., Chialvo, A. A., Cummings, P. T., Burchell, T. D., More, K. L. (2005). Effect of temperature on the adsorption of water in porous carbons. *Langmuir*, 21(21), 9457-9467.
- Talaiekhosani, A., Joudaki, S., Banisharif, F., Eskandari, Z., Cho, J., Moghadam, G., Rezania, S. (2020). Comparison of azithromycin removal from water using UV radiation, Fe (VI) oxidation process and ZnO nanoparticles. *International journal of environmental research and public health*, 17(5), 1758.
- Wahab, M., Zahoor, M., Muhammad Salman, S., Kamran, A. W., Naz, S., Burlakovs, J., Kallistova, A., Pimenov, N., Zekker, I. (2021). Adsorption-membrane hybrid approach for the removal of azithromycin from water: An attempt to minimize drug resistance problem. *Water*, 13(14), 1969.
- Xu, J., Lv, H., Yang, S. T., Luo, J. (2013). Preparation of graphene adsorbents and their applications in water purification. *Reviews in Inorganic Chemistry*, 33(2-3), 139-160.



Comparison of heavy metal concentrations in marine macroalgae of the Northern Aegean Sea, Türkiye

Fatma Koçbaş^{*1}, Saniye Türk Çulha², Ayşe Gündoğdu³, Neslihan Türkçü⁴

^{*1}Department of Biology, Faculty of Arts and Sciences, Manisa Celal Bayar University, Manisa, Türkiye

² Department of Marine Biology, Faculty of Fisheries, Izmir Katip Celebi University, Izmir, Türkiye

³ Department of Hydrobiology, Faculty of Fisheries, Sinop University, Sinop, Türkiye

⁴ Department of Hydrobiology, Faculty of Fisheries, Ege University, Izmir, Türkiye

Received : 16/12/2022

Revised : 31/01/2023

Accepted : 27/02/2023

ABSTRACT: The seven heavy metal levels were determined in marine macroalgae species from 15 stations determined from the North Aegean Sea coast. Considering the metal contents varying according to the species and region, the highest concentration determined in the study was Fe, and the lowest concentration was Cd metal. According to the green algae MPI values at the all stations, the most intense pollution was found in the Alsancak, Inciralti and Güzelbahçe stations located in the inner and middle parts of Izmir Bay. In addition, the present results were compared with the maximum allowable heavy metal values in seaweed and it was determined that the Pb values were high in some stations. In addition, this study also attempted to compare the measured values with international standards for food.

Keywords: Aegean Sea, bioindicator, heavy metal, Macroalgae, MPI, Türkiye.

INTRODUCTION

The most important problem in the world is water pollution, which is the end point of all pollution. Because of bioaccumulation, biomagnification in food chains and toxicity of the heavy metal pollution in the aquatic environment has become a worldwide, ecological, economic and health problem (Naw et al., 2020). Natural events and anthropogenic activities are the main cause of heavy metals in seawater, sediments and marine organisms worldwide (Mazur et al., 2018; Bibak et al., 2020; Corrias et al., 2020; Costa et al., 2020). Heavy metals are transported long distances by hydrological cycle and atmospheric processes (M'endez et al., 2021). The hydrological cycle of water can bring to significant pollution and exposing the aquatic ecosystems to heavy metals causing contamination of marine organisms (Corrias et al., 2020). The productive coastal zones are especially devastated by the release of innumerable contaminants through a wide range of anthropogenic activities such as unplanned urbanization, municipal wastewaters, industrialization, petrochemical complexes, mining ores, petroleum industry activities, port and shipping activity, agricultural chemicals, fish farms, heavy metals, radioactivity, tourism activities and atmospheric sources e.g. burning of fossil fuels (Naggar et al., 2018; Corrias et al., 2020; Rakib, et al., 2021; M'endez et al., 2021; Ameen et al., 2022). Aquatic ecosystems and the productive coastal zones are especially affected by heavy metals, which has become an emerging issue (Kostopoulou et al., 2013; Robin et al., 2017; Bibak et al., 2020; Arisekar et al., 2021). The distribution of heavy metal in freshwater and marine environment, macroalgae or seaweeds are used as biomonitors in water and sediment (Malea and Kevrekidis, 2014; Chakraborty et al., 2014; Naw et al., 2020; Ho and Bantoto-Kinamot, 2021). Biomonitoring with marine macroalgae has found to be a useful technique for environmental monitoring since it was first used in the early 1950s (García-Seoane et al., 2018; García-Seoane et al., 2019; García-Seoane et al., 2020; Rajaram et al., 2020). Algae and molluscs are currently among the taxonomical groups most evaluated for the use of marine organisms as biomonitoring tools (Rybak et al., 2012; Malea et al., 2015; Bonanno and Orlando-Bonaca, 2018; Corales-Ultra et al., 2019; Anbazhagan et al., 2021; Orlando-Bonaca et al., 2021). Macroalgae have the basic conditions as the most suitable bioindicator of nutrients and heavy metal accumulation in aquatic environment (Corales-Ultra et al., 2019; Anbazhagan et al., 2021; Ho and Bantoto-Kinamot, 2021).

Another usage area of algae is water filtration applications. It is also used in the removal of nutrients, organic pollutants and heavy metals from wastewater (Yalçın et al., 2012; Yılmaz et al., 2016). The most dominant polysaccharides found in the cell wall of brown algae as cellulose, alginic acid and fucoidone are alginic acid and alginates (alginic acid salts) (Dodson et al., 2015; Sahoo and Seckbach, 2015; Manev and Petkova, 2021). This alginic acid and carboxylic acid abundant in alginates are directly related to metal binding capacity and are abundant in brown algae (brown algae > green algae > red algae) (Dodson et al., 2015; Ali et al., 2020; Manev and Petkova, 2021). Moreover, the chemical composition of brown algae varies according to species, habitat and season (Ko and Wan, 2014). It contains compounds with biological activity such as laminarin, which is a product of metabolism. In addition to cellulose and alginic acid, sulfated polysaccharides are also present in the cell wall. These substances in algae offer functional groups such as hydroxyl, carboxyl, sulfate and amino. These functional groups serve as the

*Corresponding author : fatma.kocbas@cbu.edu.tr

binding site responsible for biosorption (Sun et al., 2016). The bonding of the functional groups in the algal cell wall with metal ions varies according to the algae species and metal species (Ramakrishna et al., 2005).

Concentrations of heavy metals in macroalgae of the Northern Aegean Sea were investigated to evaluate an environmental risk assessment from metals contamination in May and July 2009. This study was conducted to assess the status of 7 heavy metals (Co, Cu, Fe, Ni, Cd, Pb and Zn) in marine macroalgae in the Aegean Sea. In the present work the main aims of the study were as follows:

- to determine the concentration of Co, Cu, Fe, Ni, Cd, Pb and Zn in macroalgae (*Ulva lactuca*, *Ulva intestinalis*, *Ulva linza*, *Codium fragile*, *Cystoseira barbata*, *Padina pavonica*, *Colpomenia sinuosa*, *Corallina elongata*), samples collected from different stations of the Aegean Sea, at 15 station in 2009,
- to know the class of studied macroalgae which have the ability to accumulate more the heavy metals than the other classes,
- to compare the present results with maximal level of heavy metals authorized in seaweeds (mg kg⁻¹ dry weight)

to compare the present results with the similar studies have been carried out in the same region of the Aegean Sea.

MATERIALS AND METHODS

Study area and sampling stations

This study was carried out in fifteen stations (Akcaay, Oren, Ayvalık Cunda Port, Ayvalık, Dikili Port, Çandarlı Port, Çandarlı, Aliğa Port, Aliğa PETKİM, İzmir Karşıyaka, İzmir Turan, İzmir Alsancak, İzmir Inciraltı, İzmir Güzelbahçe, İzmir Çeşme Ilıca) of the Aegean Sea (Türkiye) (Figure1). The sampling sites in this study were selected the four bays (İzmir, Çandarlı, Dikili and Edremit Bay) within the Aegean Sea. Sampling stations within the study area present different degree of trace element inputs of anthropogenic origin such as industrial activities, tourism, shipping, shipbreaking area, and fishing activities (Table 1).

Sampling materials

Macroalgae were collected from May to July 2009 from the fifteen sampling stations on coastal zone of North Aegean Sea. The sampling marine algae species were; green algae (*Ulva lactuca*, *Ulva intestinalis*, *Ulva linza*, *Codium fragile*), brown algae (*Cystoseira barbata*, *Padina pavonica*, *Colpomenia sinuosa*), red algae (*Corallina elongata*).

Chemical analyses

The macroalgae were collected by hand directly. About 500 g of the fresh weight were harvested at low tide. The samples were rinsed to remove sand, mud and epiphyte in the sea water and then with tap water and distilled water. Then they were dried at 60°C to a constant weight and homogenized manually in porcelain mortar into powder. 0.5 g of dried macroalgae samples was digested in Teflon vessels with 10 mL analytical ultrapure HNO₃ (Merck) using a microwave oven (MARS5 Microwave Digestion System-CEM Corporation). The microwave was programmed on a 20 min ramp, for macroalgae samples 15 min at 200°C and potency of 1200 W. Three replicate subsamples of each sample were processed. All procedure of the method (Method 3051A) was similar to that previously described (USEPA, 2007, UNEP, 1984). Macroalgae samples were diluted with ultrapure Milli-Q water to a final volume of 25 mL and analyzed via ICP-MS. The concentration of the heavy metals were determined by ICP-MS. Standard solutions were prepared from stock solutions (Merck, multi-element standard). Certified Reference Material BCR-279 sea lactuca (*Ulva lactuca*) (powder) was used for calibration. The results showed good agreement between certified and analytical values (recovery rates 90-110%).

The heavy metal content of algae at fifteen stations investigated in this study was compared on a regional and algae basis using the Metal Pollution Index (MPI) calculated with the formula for algae (Usero et al., 1997).

$$MPI = (C_1 \times C_2 \times \dots \times C_n)^{1/n}$$

Where: C_n are the average concentration of trace metals (n) in algae

If this combined index is above 1 the concentrations of trace metals would be considered elevated and ecosystem could be regarded as "polluted" (Teodorovic et al., 2000).



Figure 1. Sampling stations

Table 1. Coordinates and characteristics of sampling stations

Sampling stations	Coordinates	Pollution sources of sampling stations
Akçay	N39° 34.990' E 026° 55.395'	Tourism, fishing activities
Oren	N39° 29.057' E 026° 55.742'	Tourism, fishing activities
Ayvalık Cunda Port	N39° 19.591' E 026° 37.168'	Tourism, fishing activities, shipping
Ayvalık	N39° 16.481' E 026° 39.469'	Tourism, fishing activities, shipping
Dikili Port	N39° 04.246' E 026° 53.180'	Tourism, fishing activities, shipping
Çandarlı Port	N38° 55.762' E 026° 55.933'	Tourism, fishing activities, shipping
Çandarlı	N38° 56.404' E 026° 56.152'	Tourism, fishing activities, shipping
Aliğa Port	N38° 48.359' E 026° 58.393'	Industrial activities, refinery, shipping, shipbreaking area, fishing activities
Aliğa PETKIM	N38° 48.455' E 026° 57.766'	Industrial activities, refinery, shipping, shipbreaking area, fishing activities
İzmir Karşıyaka	N38° 28.960' E 027° 04.856'	Urbanization, shipping
İzmir Turan	N38° 28.070' E 027° 09.522'	Urbanization, shipping
İzmir Alsancak	N38° 25.248' E 027° 07.511'	Urbanization, shipping
İzmir İnciraltı	N38° 24.712' E 027° 01.968'	Urbanization, shipping, fishing activities
İzmir Güzelbahçe	N38° 21.382' E 026° 18.521'	Urbanization, shipping, fishing activities
İzmir Çeşme Ilıca	N38° 19.382' E 026° 18.077'	Tourism, Fishing activities

RESULTS AND DISCUSSION

The eight species of North Aegean Sea coast algae were examined for their accumulation ability in the uptake of different metals from the Turkish aquatic environment. A wide range of metal retention capacity among the different species was observed. The collected seaweed genera are listed as per sampling station, and the concentration values of the metals are summarized in Table 2.

The heavy metals accumulated in different algal taxa were: in green algae (*U. intestinalis*, *U. linza*, *U. lactuca*, *C. fragile*), Fe > Zn > Cu > Ni > Co > Pb > Cd; in brown algae (*P. pavonica*, *C. barbata*, *C. sinuosa*), Fe > Cu > Zn > Ni > Co > Pb > Cd;

Heavy Metal Concentrations in Marine Macroalgae

in red algae (*C. elongata*) $Fe > Zn > Cu > Ni > Co > Pb = Cd$. The Cd concentrations in tested macro algae samples were found to be below the lower limit detection (<0.01). In this study, high levels of Fe were detected in almost all the specimens tested, especially, *U. intestinalis* and *U. linza* in green algae, reaching a concentration higher than the other species. Algae belonging to the Chlorophyceae (*U. intestinalis* and *U. linza*) from the North Aegean Sea generally accumulated most elements.

The biomass concentration is another important variable during metal uptake. At a given equilibrium concentration, the biomass takes up more metal ions at lower than at higher cell densities (Mehta and Gaur, 2001). It has been suggested that electrostatic interactions between cells can be a significant factor in the relationship between biomass concentration and metal sorption. In this connection, at a given metal concentration, the lower the biomass concentration in suspension, the higher will be the metal/biosorbent ratio and the metal retained by sorbent unit, unless the biomass reaches saturation. High biomass concentrations can exert a shell effect, protecting the active sites from being occupied by metal. The result of this is a lower specific metal uptake, that is, a smaller amount of metal uptake per biomass unit (Romera et al., 2007). The highest uptake in macroalgae species at the sampling sites were as follows: **Cu** in *C. sinuosa*, *U. linza*, *U. intestinalis*, *P. pavonica*, **Co** in *U. lactuca*, *U. linza*, *P. pavonica*, **Zn** in *U. linza*, *U. lactuca*, *U. intestinalis*, **Fe** in *C. sinuosa*, *U. intestinalis*, Ni in *U. intestinalis*, *C. sinuosa*, *U. lactuca*, **Pb** in *U. linza*, and *P. pavonica*. Heavy metal levels of *C. sinuosa*, *U. intestinalis* and *U. linza* were significantly higher than those in other marine algae species. The highest levels of heavy elements were found in *C. sinuosa* collected from Ören, with concentrations up to $5667.3 \mu\text{g g}^{-1}$ for Fe. Studies performed in other Aegean Sea Coast revealed that the concentration of heavy metals in macroalgae is at high levels of Fe (Tunçer, 1989; Türkan et al., 1989; Uysal, 1992; Çetingül and Aysel, 1998; Akçalı and Küçüksezgin, 2009).

The information acquired in this preliminary investigation supports of the assumption on the selective ability of macroalgae to accumulate inorganic contaminants from seawater. The concentration of trace elements in macro algae samples range widely, from $<0.01 \mu\text{g g}^{-1}$ (Cd) to $5667.3 \mu\text{g g}^{-1}$ (Fe). This situation is supported by the results of other studies (Farias et al., 2002). Compared to metals accumulation; high levels of Fe and Cu were found in *C. sinuosa* collected from Oren, high levels of Co were found in *U. lactuca* collected from Turan, high levels of Ni were found in *U. intestinalis* collected from Akçay, high levels of Zn were found in *U. linza* collected from Güzelbahçe (Table 2). Biological, physical and chemical conditions affect both the distribution and the role of the elements, compounds and residues in a system. Furthermore, seaweeds have a high potential capacity for storing trace metals, depending on the species of alga and the metal. Previous studies have shown that members of the macroalgae have the high capacity for storing metals (Rodriguez-Castaneda et al., 2006). This study shows that concentrations of elements in the macroalgae collected in the Aegean Sea and the world vary depending on species and sampling area (Table 3), probably because many variables affect the accumulation of elements in algae including the abundance of these elements in the local environmental conditions, and by a species particular metabolic processes (Försberg et al., 1988; Rodriguez-Castaneda et al., 2006).

The green macroalgae *U. lactuca* was the most widespread in the area of the sample, being found in 10 stations. Therefore, *U. lactuca* is selected that compare levels of heavy metal accumulation is thought to be appropriate. The variations in the concentrations of these elements in the *U. lactuca* can be related to the influence of territorial factors such as naturally resulting higher contents of heavy metals in the water and sediments of certain parts of the Aegean Sea. The area has been subject to very high levels of pollution due to industrial activity, municipal wastewaters, agricultural chemicals, oil pollution and airborne particles. The macroalgae species are usually used to indicate heavy metal levels in both estuarine and coastal waters throughout the world. In benthic food webs, macroalgae are key links and they act as time-integrators of pollutants (Türk Çulha et al., 2010). This study compared the amount of the metals. The relative abundance of the heavy metals was always the following $Fe > Zn > Cu$ ($5667.3, 93.52, 51.18 \mu\text{g g}^{-1}$, respectively). An analogous sequence is reported in other paper concerning metal distribution in seaweeds (Türkan et al., 1989; Ganesan et al., 1991; Uysal, 1992; Rajendran et al., 1993; Çetingül and Aysel, 1998; Malea and Haritonidis, 1999; Caliceti et al., 2002). In algae species collected from all stations, while the lowest level of Pb and Cd were also measured.

The MPI was calculated to compare the total metal concentrations in the algae of fifteen different stations (Table 2, Figure 2). The MPI values determined according to the seven metals detected in all algae sampled from each station are as follows; Oren (6.89) > Akçay (6.18) > Ayvalık Cunda (4.73) > Alsancak (3.49). MPI values in the green algae seaweed species are summarized in Figure 3. The MPI values determined according to the green algae species found in other stations except Çeşme Ilıca station are as follows; Alsancak (3.49) > Güzelbahçe (2.69) > Inciraltı (2.63). According to the data obtained from the study, it was determined that the metal distributions in the stations differed. The higher metal content in the algae species sampled from these 4 stations is related to the amount of metal in the water, the form of the metal (ion, compound, dissolved, etc.) and the presence of the metal. It differs in metal concentrations in sampling stations compared to green algae. It has been determined that MPI values are high because the sampling stations with the highest metal concentrations are located in Izmir Inner and Middle Bay. Studies have shown that algae is a good indicator species for detecting heavy metals in the environment (Rakib et al., 2021).

Table 2. Average heavy metal concentrations (mg kg^{-1} dry weight) in marine algae samples of all sampling stations in the North Aegean Sea

Stations	Species	Cd	Pb	Co	Cu	Ni	Zn	Fe	MPI
Akçay	<i>U. lactuca</i>	<0.01	<0.01	1.31	34.34	13.71	1.63	467.54	6.18
	<i>C. barbata</i>	<0.01	<0.01	1.44	22.85	6.24	10.28	340.73	
	<i>P. pavonica</i>	<0.01	2.34	2.90	11.98	10.10	41.20	2380.74	
Oren	<i>U. intestinalis</i>	<0.01	6.30	0.40	31.26	17.97	21.36	4146.66	6.89
	<i>C. barbata</i>	<0.01	<0.01	1.50	32.36	3.18	10.22	640.32	
	<i>P. pavonica</i>	<0.01	1.94	1.64	34.50	3.73	18.77	1034.46	
	<i>C. sinuosa</i>	<0.01	9.31	5.68	60.70	16.86	54.77	5667.30	
	<i>U. linza</i>	<0.01	14.01	2.45	39.12	1.93	10.81	280.84	
Ayvalık-Cunda Port	<i>U. lactuca</i>	<0.01	<0.01	<0.01	26.12	1.34	1.67	330.37	4.73
	<i>C. barbata</i>	<0.01	1.52	<0.01	18.33	<0.01	13.21	528.41	
	<i>U. lactuca</i>	<0.01	<0.01	1.72	34.53	1.76	11.25	457.07	
	<i>U. intestinalis</i>	<0.01	<0.01	1.17	24.27	2.83	11.51	972.30	
	<i>P. pavonica</i>	<0.01	11.4	0.19	31.50	1.51	44.68	1699.32	
Ayvalık	<i>U. linza</i>	<0.01	1.89	1.00	51.18	3.22	75.97	2132.94	2.00
	<i>C. barbata</i>	<0.01	<0.01	1.76	23.82	2.32	45.60	838.74	
	<i>U. intestinalis</i>	<0.01	<0.01	0.98	42.53	2.32	10.53	924.42	
	<i>P. pavonica</i>	<0.01	<0.01	<0.01	44.22	0.66	35.93	1738.08	
	<i>U. lactuca</i>	<0.01	<0.01	1.57	23.95	<0.01	0.35	1140.54	
Izmir/Dikili Port	<i>U. intestinalis</i>	<0.01	<0.01	2.82	34.87	<0.01	36.43	647.58	1.78
	<i>C. barbata</i>	<0.01	<0.01	<0.01	14.96	2.77	2.71	519.64	
Izmir/Çandarlı Port	<i>U. lactuca</i>	<0.01	<0.01	1.97	9.14	0.24	0.53	739.74	0.85
	<i>U. linza</i>	<0.01	<0.01	1.54	7.11	2.69	0.12	221.38	
Izmir/Çandarlı	<i>U. lactuca</i>	<0.01	<0.01	1.42	9.26	0.34	4.37	546.18	1.37
	<i>U. intestinalis</i>	<0.01	<0.01	<0.01	7.77	2.96	22.46	768.72	
Izmir/Aliağa Port	<i>U. intestinalis</i>	<0.01	<0.01	<0.01	4.44	2.37	61.10	539.32	0.83
	<i>C. elongata</i>	<0.01	<0.01	<0.01	8.54	7.43	11.51	299.46	
Izmir/Aliağa PETKİM	<i>U. lactuca</i>	<0.01	<0.01	0.49	7.93	6.36	12.69	304.76	2.26
	<i>C. elongata</i>	<0.01	<0.01	2.16	37.94	9.69	71.97	2297.52	
	<i>C. fragile</i>	<0.01	<0.01	<0.01	2.93	1.64	16.14	526.57	
Izmir/Karşıyaka	<i>U. linza</i>	<0.01	<0.01	14.38	10.26	1.67	39.83	77.50	1.86
Izmir/Turan	<i>U. lactuca</i>	<0.01	<0.01	15.96	10.76	<0.01	29.46	885.72	1.24
Izmir/Alsancak	<i>U. intestinalis</i>	<0.01	<0.01	8.91	19.42	8.19	72.04	608.16	3.49
Izmir/İnciraltı	<i>U. lactuca</i>	<0.01	<0.01	12.69	15.49	2.72	19.30	827.04	2.63
Izmir/Güzelbahçe	<i>U. intestinalis</i>	<0.01	<0.01	4.52	6.66	3.83	32.20	454.89	2.15
	<i>U. lactuca</i>	<0.01	<0.01	10.48	11.48	2.85	81.34	364.91	
	<i>U. linza</i>	<0.01	<0.01	1.93	1.57	<0.01	93.52	295.28	
Izmir/Çeşme-İlca	<i>P. pavonica</i>	<0.01	<0.01	12.32	18.16	<0.01	20.82	1450.80	1.31

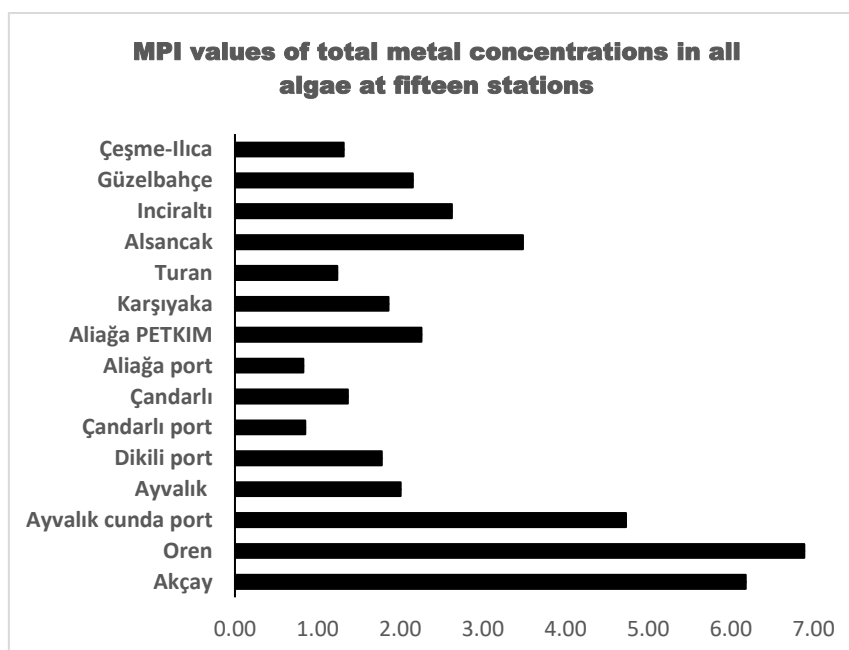
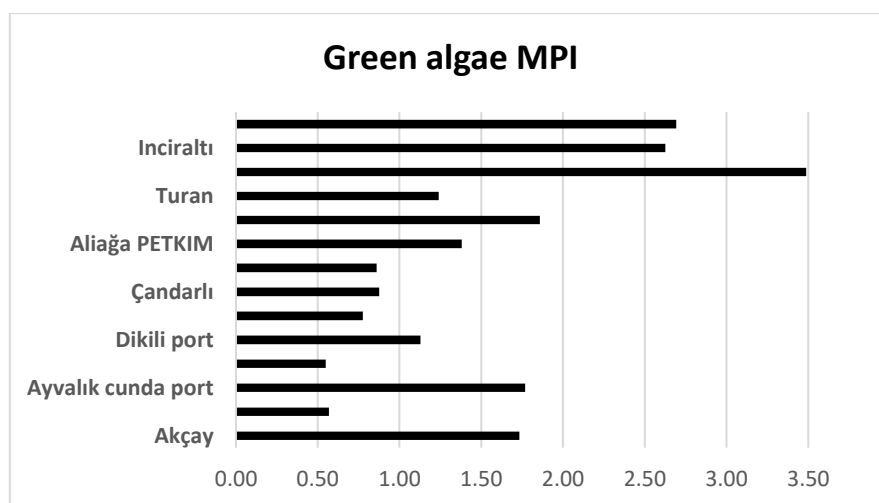
**Figure 2.** MPI values of total metal concentrations in all algae at fifteen stations

Table 3. Comparison of heavy metal distribution in marine algae of Türkiye and in the world ($\mu\text{g g}^{-1}$ dry weight).

Species	Sites	Fe	Zn	Cu	Pb	Cd	Ref.
<i>U. lactuca</i>	Izmir and Çandarlı Bay (Türkiye)	34.30-583.80	3.20-37.13	0.39-6.22	0.29-8.40	0.01-0.60	1
<i>Ulva</i> sp.	Izmir Bay (Türkiye)	458-1300	32-80	39.67	31-132	0.56-1.06	2
<i>Ulva</i> sp.	Izmir Bay (Türkiye)	--	8.02	1.82	3.31	0.13	3
<i>Ulva</i> sp.	Aegean Sea (Türkiye)	223-1331	9.10-29.50	1.30-15.34	0.54-3.07	0.42-3.00	4
<i>C. barbata</i>	Izmir Bay (Türkiye)	258-15060	31.2-150	4.60-56.50	0.0-30.0	0.30-2.40	5
<i>P. pavonina</i>	Izmir and Çandarlı Bay (Türkiye)	40.70-345.20	3.7-35.40	0.50-2.60	1.50-9.86	0.06-0.72	1
<i>Cystoseira</i> sp.	Izmir/Foça (Türkiye)	97.62	10.81	3.78	0.01	0.0052	6
<i>Cystoseira</i> sp.	Izmir/Urla (Türkiye)	212.14	27.17	2.25	0.01	0.19	7
<i>Codium</i> sp.	Izmir Bay (Türkiye)	--	4.89	0.92	3.13	0.14	8
<i>Codium bursa</i>	Izmir Bay (Türkiye)	--	1.98	0.63	1.64	0.18	8
<i>C. barbata</i>	Ayvalık (Türkiye)	--	4.36-7.95	3.12-7.87	20.7-67.44	<0.001	9
<i>P. pavonica</i>	Ayvalık (Türkiye)	--	0.28-3.09	6.95-10.85	24.20-45.35	<0.001	9
<i>Ulva</i> sp.	Coast of Istanbul (Türkiye)	88.74	6.92	4.92	0.26	0.05	10
<i>U. intestinalis</i>	Kadın Creek (Gokova Bay/Türkiye).	--	7.20-68.22	1.50-38.95	2.49-8.02	0.01-0.19	11
<i>C. fragile</i>	Thessaloniki Gulf, Aegean Sea (Greece)	--	105.96	5.07	3.89	0.046	12
<i>U. lactuca</i>	Iskenderun and Mersin Bay (Turkey)	5828.50	129.0	29.56	12.09	0.24	13
<i>P. pavonica</i>	Iskenderun and Mersin Bay (Turkey)	777.90	25.48	8.01	5.89	0.24	13
<i>Cystoseira corniculata</i>	Iskenderun and Mersin Bay (Turkey)	236.23	31.03	10.79	5.83	0.24	13
<i>U. lactuca</i>	Black Sea (Turkey)	1754	--	--	0.08-1.90	0.09-0.66	14
<i>U. linza</i>	Black Sea (Turkey)	--	7	--	--	--	14
<i>C. barbata</i>	Black Sea (Turkey)	327	65	5-37	--	--	14
<i>U. intestinalis</i>	Sürmene Bay (Turkey)	--	351.50	493.00	15.80	--	15
<i>Corallina officinalis</i>	Aegean Sea (Greece)	--	37.50	0.85	0.02	2.90	16
<i>U. lactuca</i>	Gulf of Gaeta (Italy)	--	37-54	4.9-6.4	1.67-2.28	0.13-0.21	17
<i>U. intestinalis</i>	Thessaloniki Gulf, (Greece)	--	122.8	9.15	4.62	0.03	12
<i>P. pavonica</i>	Gulf of Gaeta (Italy)	--	45-56	11.8-13.2	0.34-4.82	0.39-0.66	17
<i>U. lactuca</i>	Suez Gulf (Egypt)	464.10	22.35	5.70	8.69	0.66	18
<i>U. lactuca</i>	Suez Canal (Egypt)	628.00	13.90	8.92	7.19	0.59	18
<i>Ulva</i> sp.	Alexandria region (Egypt)	687.60	12.63	11.71	4.96	0.31	19

*Ref: 1. Tunçer, 1989; 2. Türkan et al., 1989; 3. Küçüksezgin and Balcı, 1994; 4. Uysal, 1992; 5. Çetingül and Aysel, 1998; 6. Akçalı and Küçüksezgin, 2009; 7. Akçalı and Küçüksezgin, 2009; 8. Küçüksezgin and Balcı, 1994; 9. Koçbaş et al., 2018; 10. Özden et al., 2019; 11. Yozokmaz et al., 2018; 12. Malea et al., 2015; 13. Erguden et al., 2021; 14. Arici and Bat, 2016; 15. Alkan et al., 2020; 16. Sawadis et al., 2001; 17. Conti and Cecchetti, 2003; 18. Mourad and El-Azim, 2019; 19. Saeed and Moustafa, 2013.

**Figure 3.** Metal pollution index (MPI) for the fourteen station in the green seaweed species investigated

On the basis of our results we conclude that the Aegean Sea has suffered seriously from human impacts, and that the characteristics of this region encourage a natural increase in certain elements in the sediments and water, which is then reflected in the macroalgae. During each algal genera assorted in its ability to uptake and accumulate individual metals, general accumulation tendencies were still evident across all genera of algae. On the basis of the levels of heavy metals observed its wide distribution in the North Aegean Sea, this organism achieves a number of preconditions to be considered as an adequate biomonitor for future studies. Results obtained so far from macroalgae collected in the coastal waters of Aegean Sea demonstrate that there is localized variation in each of the different areas, and that the accumulation of some elements is probably identified by their relative concentration in the surrounding water and sediments, by a species' particular metabolic processes, and by local environmental conditions.

Moreover, maximum allowed levels of heavy metal have been defined for edible seaweed (Table 4). According to CEVA (Centre d'Étude et de Valorisation des Algues) (2014)'s maximum limit in consumable algae, values; *U. intestinalis* from Green algae at Akçay station, *U. linza* from Green algae at Oren station, *C. sinuosa* from Brown algae and pavonica from Brown algae sampled from Ayvalık-Cunda Port station were found to be well above the limit values for Pb consumption. Since these algae are not consumed as food in Türkiye, they do not effect any health risk.

Table 4. Maximal level of heavy metals and iodine authorized in seaweeds (mg kg^{-1} dry weight) (CEVA, 2014)

Elements	Max. Level (mg kg^{-1} dry weight)
Inorganic Arsenic (As)	3
Cadmium (Cd)	0.5
Mercury (Hg)	0.1
Lead (Pb)	5
Tin (Sn)	5
Iodine (I)	2000

CONCLUSION

Our results showed that Fe, Ni, Cu, Co and Zn concentrations are higher, but Pb and Cd levels are lower than in the same macroalgae species collected from the Aegean Sea in 2009. A comparison of the present results with data reported for similar macroalgae species from other Turkish marine environment, suggest that the heavy metal levels are higher in the Aegean macroalgae than Bosphorus and Marmara Sea, Mediterranean and Black Sea macroalgae. It has been determined that the macroalgae species examined in this study in the North Aegean Sea are good indicator species in determining environmental pollution. Compared to other seas, heavy metal concentrations determined in Aegean Sea macroalgae are quite high. Since these marine macroalgae are not consumed as food in Turkey, they do not pose any health risk. In future research, it is necessary to examine in more detail the exportable and consumable marine macroalgae in terms of heavy metal accumulation and to determine the maximum consumable limit values for Türkiye.

CONFLICT OF INTEREST

No conflict of interest was declared by the authors.

REFERENCES

- Akçalı, İ., Küçüksezgin, F. (2009). Bioaccumulation of heavy metals by the brown algae *Cystoseira* sp. along the Aegean Sea. E.U. Journal of Fisheries & Aquatic Sciences, 26(3), 159-163.
- Alkan, N., Alkan, A., Demirak, A., Bahloul, M. (2020). Metals/metalloid in marine sediments, bioaccumulating in macroalgae and a mussel, soil and sediment contamination. An International Journal, 29(5), 569-594. [doi:10.1080/15320383.2020.1751061](https://doi.org/10.1080/15320383.2020.1751061).
- Ali, H.S., Kandil, N.F.E.S., Ibraheem, I.B.M. (2020). Biosorption of Pb^{2+} and Cr^{3+} ions from aqueous solution by two brown marine macroalgae: An equilibrium and kinetic study. Desalination and Water Treatment, 206, 250–262.
- Ameen, F., Al-Homaidan, A. A., Almahasheer, H., Dawoud, T., Alwakeel, S., AlMaarofi, S. (2022). Biomonitoring coastal pollution on the Arabian Gulf and the Gulf of Aden using macroalgae: A review. Marine Pollution Bulletin. 175, 113156. [doi: 10.1016/j.marpolbul.2021.113156](https://doi.org/10.1016/j.marpolbul.2021.113156).

- Anbazhagan, V., Partheeban, E.C., Arumugam, G., Arumugam, A., Rajendran, R., Paray, B. A., Al-Sadoon, M.K., Al-Mfarij, A.R. (2021). Health risk assessment and bioaccumulation of metals in brown and red seaweeds collected from a tropical marine biosphere reserve. *Marine Pollution Bulletin*, 164, 112029. doi: [10.1016/j.marpolbul.2021.112029](https://doi.org/10.1016/j.marpolbul.2021.112029).
- Arici, E., Bat, L. (2016). Using marine macroalgae as biomonitors: heavy metal pollution along the Turkish west coasts of the Black Sea. 41st CIESM Congress, Kiel (Germany), 12-16 September 2016. *Rapp. Comm. Int. Mer Medit.At: Kiel (Germany)* Vol. 41, 238.
- Arisekar, U., Shakila, R.J., Shalini, R., Jeyasekaran, G., Sivaraman, B., Surya, T. 2021. Heavy metal concentrations in the macroalgae, seagrasses, mangroves, and crabs collected from the Tuticorin coast (Hare Island), Gulf of Mannar, South India. *Marine Pollution Bulletin*, 163, 111971.
- Bibak, M., Sattari, M., Tahmasebi, S., Agharokh, A., Nami, J.I. (2020). Marine macro-algae as a bio-indicator of heavy metal pollution in the marine environments, Persian Gulf. *Indian Journal of Geo Marine Sciences*, 49 (03), 357-363.
- Bonanno, G., Orlando-Bonaca, M. (2018). Trace elements in Mediterranean seagrasses and macroalgae. A review. *Science of the Total Environment*, 618, 1152–1159. doi: [10.1016/j.scitotenv.2017.09.192](https://doi.org/10.1016/j.scitotenv.2017.09.192).
- Caliceti, M., Argese, E., Sfriso, A., Pavoni, B. (2002). Heavy metal contamination in the seaweeds of the Venice lagoon. *Chemosphere*, 47, 443 – 454.
- CEVA (Centre d'Étude et de Valorisation des Algues) 2014. Edible seaweed and French regulation-Synthesis made by CEVA, 3 pp.: www.ceva.fr/. Available 09.11.2021.
- Chakraborty, S., Bhattacharya, T., Singh, G., Maity, J.P. (2014). Benthic macroalgae as biological indicators of heavy metal pollution in the marine environments: A biomonitoring approach for pollution assessment. *Ecotoxicology and Environmental Safety*, 100, 61–68. doi: [10.1016/j.ecoenv.2013.12.003](https://doi.org/10.1016/j.ecoenv.2013.12.003).
- Conti, M.E., Cecchetti, G. (2003). A biomonitoring study: trace metals in algae and molluscs from Tyrrhenian coastal areas. *Environmental Research*, 93, 99–112. doi: [10.1016/S0013-9351\(03\)00012-4](https://doi.org/10.1016/S0013-9351(03)00012-4).
- Corales-Ultra, O.G., Peja Jr, R.P., Casas Jr, E.V. (2019). Baseline study on the levels of heavy metals in seawater and macroalgae near an abandoned mine in Manicani, Guiuan, Eastern Samar, Philippines. *Marine Pollution Bulletin*, 149, 110549. doi: [10.1016/j.marpolbul.2019.110549](https://doi.org/10.1016/j.marpolbul.2019.110549).
- Corrias, F., Atzei, A., Addis, P., Secci, M., Russo, M., Angioni, A. (2020). Integrated environmental evaluation of heavy metals and metalloids bioaccumulation in invertebrates and seaweeds from different marine coastal areas of Sardinia, Mediterranean Sea. *Environmental Pollution*, 266, 115048. doi: [10.1016/j.envpol.2020.115048](https://doi.org/10.1016/j.envpol.2020.115048).
- Costa, G.B., Koerich, G., de Ramos, B., Ramlov, F., Martínez-Crego, B., Costa, M.M., Jesus, D., Santos, R.O.P., Horta Jr, P.A. (2020). A review of common parameters and descriptors used in studies of the impacts of heavy metal pollution on marine macroalgae: identification of knowledge gaps and future needs. *Acta Botanica Brasilica*, 34(3), 460-477. doi: [10.1590/0102-33062020abb0072](https://doi.org/10.1590/0102-33062020abb0072).
- Çetingül, V., Aysel, V. (1998). Heavy metal accumulation of some Brown and red algae which has economical importance. *E. U. Journal of Fisheries & Aquatic Sciences*, 15 (1-2), 63-76.
- Dodson, J.R., Parker, H.L., García, A.M., Hicken, A., Asemave, K., Farmer, T.J., He, H., Clark, J.H., Hunt, A.J. (2015). Bio-derived materials as a green route for precious & critical metal recovery and re-use. *Green Chemist*, 17(4),1951–65. doi: [10.1039/C4GC02483](https://doi.org/10.1039/C4GC02483)
- Erguden, S.A., Erguden, D., Ciftci, N., Akbora, H.D., Ayas, D. (2021). Metal levels of macroalgae from Iskenderun and Mersin Bay Turkey Eastern Mediterranean. *Fresenius Environmental Bulletin*, 30(07), 8365-8371.
- Farias, S., Arisnabarretab, S.P., Vodopivec, C., Smichowskia, P. (2002). Levels of essential and potentially toxic trace metals in Antarctic macro algae. *Spectrochimica Acta Part B*, 57, 2133–2140.
- Försberg, A., Söderlund, S., Frank, A., Petersson, L. R., Pedersén M. (1988). Studies on metal content in the brown seaweed *Fucus vesiculosus*, from the Archipelago of Stockholm. *Env. Pollut*, 49, 245 – 263.

- Ganesan, M., Kannan, R., Rajendran, K., Govindasamy, C., Sampathkumar, P., Kannan, L. (1991). Trace metal distribution in seaweeds of the Gulf of Mannar, Bay of Bengal. *Marine Pollution Bulletin*, 22 (4), 205–207.
- García-Seoane, R., Aboal, J.R., Boquete, M.T., Fernández, J.A. (2018). Biomonitoring coastal environments with transplanted macroalgae: A methodological review. *Marine Pollution Bulletin*, 135, 988–999. doi: [10.1016/j.marpolbul.2018.08.027](https://doi.org/10.1016/j.marpolbul.2018.08.027).
- García-Seoane, R., Fernandez, J.A., Varela, Z., Real, C., Boquete, M.T., Aboal, J.R. (2019). Sampling optimization for biomonitoring metal contamination with marine macroalgae. *Environmental Pollution*, 255, 113349. doi: [10.1016/j.envpol.2019.113349](https://doi.org/10.1016/j.envpol.2019.113349).
- García-Seoane, R., Aboal, J.R., Boquete, M.T., Fernández, J.A. (2020). Phenotypic differences in heavy metal accumulation in populations of the brown macroalgae *Fucus vesiculosus*: A transplantation experiment. *Ecological Indicators*, 111, 105978. doi: [10.1016/j.ecolind.2019.105978](https://doi.org/10.1016/j.ecolind.2019.105978).
- Ho, M.T.G., Bantoto-Kinamot, V. (2021). *Sargassum*, *Padina* and *Turbinaria* as bioindicators of cadmium in Bais Bay, Negros Oriental. *The Palawan Scientist*, 13(1), 90-98.
- Ko, F.K., Wan, Y. (2014). Introduction to nanofiber materials. Cambridge University Press. doi:10.1017/CBO9781139021333
- Koçbaş, F., Ay, G., Kılıç, M., Kılıç, F. (2018). Investigation of the pollution in the Ayvalık saltern with green and brown macroalgae. Agriculture, Environment and Health Congress, Aydın (Turkey).
- Kostopoulou, M., Guida, M., Nikolau, A., Oral, R., Trifuoggi, M., Borriello, I., Vagi, M., D’Ambra, Meriç, S., Pagano, G. (2013). Inorganic and organic contamination in sediment from Izmir Bay (Turkey) and Mytilene Harbor (Greece). *Global NEST Journal*, 15(1), 57-68.
- Küçüksezgin, F., Balci, A. (1994). Heavy metal concentrations in selected organisms from Izmir Bay, Turkey, *Marine Pollution Bulletin*, 28 (5), 333-335.
- M’endez, S., Ruepert, C., Mena, F., Cortés, J. (2021). Accumulation of heavy metals (Cd, Cr, Cu, Mn, Pb, Ni, Zn) in sediments, macroalgae (*Cryptonemia crenulata*) and sponge (*Cinachyrella kuekenthali*) of a coral reef in Moín, Limón, Costa Rica: An ecotoxicological approach. *Marine Pollution Bulletin*, 173, 113159. doi: [10.1016/j.marpolbul.2021.113159](https://doi.org/10.1016/j.marpolbul.2021.113159).
- Malea, P., Kevrekidis, T. (2014). Trace element patterns in marine macroalgae. *Science of the Total Environment*, 494–495, 144–157. doi: [10.1016/j.scitotenv.2014.06.134](https://doi.org/10.1016/j.scitotenv.2014.06.134).
- Malea, P., Chatziapostolou, A., Kevrekidis, T. (2015). Trace element seasonality in marine macroalgae of different functional-form groups. *Marine Environmental Research*, 103, 18-26. doi: [10.1016/j.marenvres.2014.11.004](https://doi.org/10.1016/j.marenvres.2014.11.004).
- Malea, P., Haritonidis, S. (1999). Seasonal accumulation of metals by red alga *Gracilaria verrucosa* (Hud.) Papenf. From Thermaikos Gulf, Greece. *Journal of Applied Phycology*, 11, 503 – 509.
- Mazur, L.P., Cechinel, M.A.P., Guelli U. de Souza, S.M.A., Boaventura, R.A.R., Vilar, V.J.P. (2018). Brown marine macroalgae as natural cation exchangers for toxic metal removal from industrial wastewaters: A review. *Journal of Environmental Management*, 223, 215-253. doi: [10.1016/j.jenvman.2018.05.086](https://doi.org/10.1016/j.jenvman.2018.05.086).
- Manev, Z.K., Petkova, N.T. (2021). Component composition and antioxidant potential of *Cystoseira barbata* from the Black Sea. *Bulletin of the Transilvania University of Brasov, Series II: Forestry, Wood Industry, Agricultural Food Engineering*, 14–63(1),164–72.
- Mehta, S.K., Gaur, J.P. (2001). Characterization and optimization of Ni and Cu sorption from aqueous solution by *Chlorella vulgaris*. *Ecological Engineering*, 18, 1 – 13.
- Mourad, F.A., El-Azim, H.A. (2019). Use of green alga *Ulva lactuca* (L.) as an indicator to heavy metal pollution at intertidal waters in Suez Gulf, Aqaba Gulf and Suez Canal, Egypt. *Egyptian Journal of Aquatic Biology & Fisheries*, 23(4), 437 – 449.
- Naggar, Y.A., Khalil, M.S., Ghorab, M.A. (2018). Environmental pollution by heavy metals in the aquatic ecosystems of Egypt. *Open Access Journal of Toxicology*, 3(1): doi:[10.19080/OAJT.2018.03.555603](https://doi.org/10.19080/OAJT.2018.03.555603).

- Naw, S.W., Zaw, N.D.K., Aminah, N.S., Alamsjah, M.A., Kristanti, A.N., Nege, A.S., Aung, H.T. (2020). Bioactivities, heavy metal contents and toxicity effect of macroalgae from two sites in Madura, Indonesia. *Journal of the Saudi Society of Agricultural Sciences*, 19(8), 528-537. doi:10.1016/j.jssas.2020.09.007.
- Orlando-Bonaca, M., Pitacco, V., Bajt, O., Falnoga, I., Hudobivnik, M.J., Mazej, D., Šlejkovec, Z., Bonanno, G. (2021). Spatial and temporal distribution of trace elements in *Padina pavonica* from the northern Adriatic Sea. *Marine Pollution Bulletin*, 172, 112874. doi: 10.1016/j.marpolbul.2021.112874.
- Özden, Ö., Orhan, Y., Kaplan, M., Parıldar, S., Erkan, N. (2019). Trace toxic mineral levels of sea lettuce (*Ulva* spp.) from coast of Istanbul. *Aquatic Research*, 2(3), 154-160. doi:10.3153/AR19013.
- Rajaram, R., Rameshkumar, S., Anandkumar, A. (2020). Health risk assessment and potentiality of green seaweeds on bioaccumulation of trace elements along the Palk Bay coast, Southeastern India. *Marine Pollution Bulletin*, 154, 111069. doi: 10.1016/j.marpolbul.2020.111069.
- Rakib M.R.J., Jolly, Y.N., Dioses-Salinas, D.C., Pizarro-Ortega, C.I., De-la-Torre, G.E., Khandaker, M.U., Alsubaie, A., Almalki, A.S.A., Bradley, D.A. (2021). Macroalgae in biomonitoring of metal pollution in the Bay of Bengal coastal waters of Cox's Bazar and surrounding areas. *Scientific Reports*, 11(1), 20999. doi: 10.1038/s41598-021-99750-7
- Ramakrishna, S., Fujihara, K., Teo, W. E., Lim, T. C., Ma, Z. (2005). An introduction to electrospinning and nanofibers. *An Introduction to Electrospinning and Nanofibers*. doi: 10.1142/5894.
- Rajendran, K., Sampathkumar, P., Govindasamy, C., Ganesan, M., Kannan, R., Kannan, L. (1993). Levels of trace metals (Mn, Fe, Cu and Zn) in some Indian seaweeds. *Marine Pollution Bulletin*, 26 (5), 283 – 285.
- Robin, A., Chavel, P., Chemodanov, A., Israel, A., Golberg, A. (2017). Diversity of monosaccharides in marine macroalgae from the Eastern Mediterranean Sea. *Algal Research*, 28, 118–127. doi: 10.1016/j.algal.2017.10.005.
- Rodríguez-Castaneda, A. P., Sánchez-Rodríguez, I., Shumilin, E. N., Sapozhnikov, D. (2006). Element concentrations in some species of seaweeds from La Paz Bay and La Paz Lagoon, south-western Baja California, Mexico. *Journal of Applied Phycology*, 18, 399–408.
- Romera, E., Gonzalez, F., Ballester, A., Blazquez, M. L., Munoz, J. A. (2007). Comparative study of biosorption of heavy metals using different types of algae. *Bioresource Technology*, 98, 3344 – 3353.
- Rybak, A., Messyasz, B., Łeska, B. (2012). Freshwater *Ulva* (Chlorophyta) as a bioaccumulator of selected heavy metals (Cd, Ni and Pb) and alkaline earth metals (Ca and Mg). *Chemosphere*, 89, 1066–1076. doi: 10.1016/j.chemosphere.2012.05.071.
- Saeed, S.M., Moustafa, Y.T.A. (2013). The seaweed (green macroalgae), *Ulva* sp. as bioindicator of metal pollution in the Mediterranean Coast, Alexandria region, Egypt. *Egypt. J. Aquat. Biol. & Fish.*, 17 (3), 57-68
- Sahoo, D., Seckbach, J. (2015). *The algae world*. 17(4), 1951–65, Springer. doi: 10.1007/978-94-017-7321-8.
- Sawadis, T., Brown, M.T., Zachariadis, G., Srtis, I. (2001). Trace metal concentrations in marine macroalgae from different biotopes in the Aegean Sea. *Environment International*, 27, 43-47.
- Sun, G., Sun, L., Xie, H., Liu, J. (2016). Electrospinning of nanofibers for energy applications. *Nanomaterials*, 6(7), 129.
- Teodorovic, I., Djukic, N., Maletić, S., Miljanovic, B. and Jugovac, N. (2000). Metal pollution index: proposal for freshwater monitoring based on trace metal accumulation in fish. *Tiscia*, 32, 55-60.
- Tunçer, S. (1989). Heavy metals on Eel grass (*Zostera marina*) (L) and Meadow (*Posidonia oceanica*) (L) Delile in the Bay of İzmir. *Plants and Pollutants in Developed and Developing Countries*, (Edit. M.Öztürk). 151-159.
- Türk Çulha, S., Koçbaşı, F., Gündoğdu, A., Topcuoğlu, S., Çulha, M. (2010). Heavy metal levels in macroalgae from Sinop in the Black Sea, The 39th CIESM Congress (Venice 10-14 May 2010), 239.
- Türkan, I., Öztürk, M., Sukatar, A. (1989). Heavy metal accumulation by algae in the Bay of Izmir, Turkey, *Rew. Int. Med.* 71-76.

- UNEP (United Nations Environment Programme). (1984). Determination of total Cd, Zn, Pb and Cu in selected marine organisms by flameless AAS reference methods for marine pollution studies, vol. 11.
- U.S.EPA (U.S. Environmental Protection Agency). (2007). Method 3051A(SW-846): Microwave Assisted Acid Digestion of Sediments, Sludges, and Oils. Revision 1. Washington, DC.
- Usero, J., Gonzalez-Regalado, E., Gracia, I. (1997). Trace metals in the bivalve molluscs *Ruditapes decussatus* and *Ruditapes philippinarum* from the Atlantic Coast of Southern Spain. Environ. Int, 23, 291–298. doi: [10.1016/S0160-4120\(97\)00030-5](https://doi.org/10.1016/S0160-4120(97)00030-5).
- Uysal, H. (1992). Heavy metal concentrations in selected marine species from Fisheries days of Aegean Coast, XXXes Journées Étude Pollutions, Trieste, Italy, CIESM.
- Yalçın, S., Sezer, S., Apak, R. (2012). Characterization and lead(II), cadmium(II), nickel(II) biosorption of dried marine brown macro algae *Cystoseira barbata*. Environmental Science and Pollution Research, 19, 3118–3125.
- Yılmaz, H.K., Dikbaş, M.D., Bilgüven, M. (2016). Pigment substances and usage areas from cyanobacteria. Journal of Agricultural Faculty of Uludag University, 30(1).
- Yozukmaz, A., Yabanlı, M., Sel, F. (2018). Heavy metal bioaccumulation in *Enteromorpha intestinalis*,(L.) Nees, a macrophytic algae: the example of Kadin Creek (Western Anatolia). Brazilian Archives of Biology and Technology. V.61: e18160777. doi:[10.1590/1678-4324-2018160777](https://doi.org/10.1590/1678-4324-2018160777)



Investigation of the antifungal activities of cryogels for potential use as wound dressing materials

Koray Şarkaya^{*1}, Berna Kavakçioğlu Yardımcı², Ayşenur Güler³

^{*1}Department of Chemistry, Faculty of Sciences, Pamukkale University, Denizli, Türkiye

² Department of Chemistry, Graduate School of Natural and Applied Sciences, Pamukkale University, Denizli, Türkiye

Received : 16/12/2022

Revised : 31/01/2023

Accepted : 27/02/2023

ABSTRACT: The fungus can act as a pathogen and disrupt the immune system. Therefore, materials with antifungal properties can provide an essential deterrent against fungal infections. The eukaryotic yeast cell model *Saccharomyces cerevisiae*, known as baker's yeast, is widely used in food industry in baking, winemaking, and brewing. Moreover it is also commonly used as a probiotic for treating gastroenteritis and regulating the endogenous flora and immune system. However, in recent years, there has been an increase in cases of fungemia caused by *S. cerevisiae* and its subspecies, *S. boulardii*, and therefore caution should be exercised when using it as probiotic especially in immunocompromised individuals or low weight infants. Cryo-hydrogels, called cryogels, are mainly used in biotechnological fields due to their fast mass flow properties supported by the elastic morphological structures combined with mechanical and chemical stability. Also, these polymers are a valuable option for wound-healing materials. In this study, HEMA-based cryogels containing different amounts of N-Vinylformamide were prepared and characterized to investigate their anti-fungal activities on *Saccharomyces cerevisiae*. The results indicated that, PHEMA/PNVF cryogels showed considerable effectiveness against this opportunistic strain. So, PHEMA/PNVF can be considered a potential wound dressing material for future studies

Keywords: Cryogels, fungemia, anti-fungal activity, *Saccharomyces cerevisiae*.

INTRODUCTION

Hydrogels are cross-linked, three-dimensional network polymers that swell without dissolving in water. Hydrogels show remarkable similarities to living tissues due to many physical properties, such as having plenty of water in their structures, biocompatibility, and being soft and flexible (Manzoor et al., 2022). Cryogels can be called cryo-hydrogels, a member of a gels family, synthesized at temperatures below the solvent's freezing point (Lozinsky, 2018). Cryogels, as compared to traditional hydrogels, have large pore sizes, more swelling ratios, a short diffusion path, good biocompatibility, also high mechanical and physical stability (Su and Okay, 2019). So, in recent years, cryogels have been preferred over hydrogels (Karacan and Okay, 2013). Cryogels can be prepared in different shapes (cylindrical, sphere, etc.), sizes (macro- or micro-), or functions such as columns or membranes (Çetin and Denizli 2019). Cryogels have a wide range of applications covering the fields of insulation, environment (Şarkaya et al., 2018), food (Coria-Hernández et al., 2018), health (Shih et al., 2018), electronics (Sevgül Bakay et al., 2022), and drug biotechnology (Ferreira et al., 2019).

The fungus has a disruptive impact on the immune system and can act as an infection. It is believed that substances having antifungal characteristics can act as a crucial deterrent against fungus infections (Zumbuehl et al., 2007). Developing new materials with antimicrobial activity has become necessary with the prevalence of microbial infections as diseases impaired wound healing and biomedical implant failure. Also, there is an increasing need for materials that can resist these negativities and have antifungal properties (Ailincai et al., 2016). In recent years, materials for wound dressing have been developed to combat pathogens' growing resistance, which can result in serious infections, challenging wound healing, and the loss of many lives (Zhao et al., 2017). Hydrogels, a class of highly hydrated biomaterials produced naturally or synthetically, can be a helpful starting point for designing antimicrobial materials (Veiga and Schneider, 2013). Before considering hydrogels as a wound dressing material for fungi infections, we aim to investigate the antifungal activities of cryogels in this study. For this purpose, we prepared 2-Hydroxyethyl Methacrylate (HEMA)-based cryogels. PHEMA cryogels are highly hydrophilic with a high swelling degree, biocompatible, hydrolytic, and chemically stable. From this point of view, PHEMA can be used as a tissue scaffold in medicine and controlled drug release systems (Roointan et al. 2018), soft contact lenses (García-Millán et al., 2015), and tissue engineering (Dragusin et al., 2012). PHEMA-based materials are tolerant of embedded cells (García-Uriostegui et al., 2018). Also, PHEMA cryogel is hardly self-degrading because of its high biostability (Moghadam and Pioletti, 2016).

Saccharomyces cerevisiae, commonly referred to as baker's yeast and used in the bread sector, is also employed as a probiotic for treating gastroenteritis and controlling the immune system and endogenous flora (Nash et al., 2017). Although it is a rare source of infection in people and is a member of the human fungal microbiome, the usage of it as probiotics in immunocompromised people have recently increased, the incidences of fungemia caused by this strain. It is noted that it should

only be used cautiously in sick patients and newborns who are underweight (McFarland, 2010). Additionally, since the critical study by Munoz et al., it has been accepted that *S. cerevisiae* fungemia may occur after using probiotics containing *S. boulardii*. In their work, it was convincingly shown that strains isolated from a patient's blood and strains isolated from the probiotic preparation were genetically identical; this is an observation that supports the hypothesis of translocation from the gut to the bloodstream (Muñoz et al., 2005).

In this study, PHEMA cryogels were selected as main monomer based on their high degree of hydrophilicity, biocompatibility, and cell-trap tolerance (García-Uriostegui et al., 2018). N-Vinylformamide (NVF), on the other hand, was utilized to produce a copolymerization reaction with HEMA. One of the most popular monomers, acrylamide, has an isomer called NVF. NVF has stronger reactivity than acrylamide and is water soluble, giving it a wider range of applications thanks to its low toxicity (Shi et al., 2008; Luo et al., 2021). As a result, polymers including NVF can be employed in many of the same applications as acrylamides (Suekama et al. 2013). In this study, PHEMA/PNVF cryogels were synthesized, characterized and the anti-fungal activities of these cryogels were investigated against wild type yeast strain of *Saccharomyces cerevisiae*. The results showed that these PHEMA/PNVF cryogels have significant antifungal effects and should be evaluated for their further applications as antifungal materials.

MATERIALS AND METHODS

2-Hydroxyethyl methacrylate (HEMA) , N-Vinyl formamide (NVF), N,N'-methylene bisacrylamide (MBAAm), Tetramethylethylenediamine (TEMED) and Ammonium persulfate (APS) were purchased from Sigma (Sigma Chemical Co., USA). All chemical reagents were of analytical purity. Ultra distilled water was used in the experiments.

Preparation of cryogels

Our previous work has precisely stated the procedure for synthesizing cryogels (Şarkaya and Allı 2021a; Şarkaya et al. 2022). According to this, 1.3 mL of HEMA was dissolved in 5 mL water, and 0.2 g of MBAAm was dissolved in 10 mL water. The two solutions are then mixed. 20 mg APS was added to the mixture and thoroughly dissolved. Solutions containing varying amounts of N-Vinylformamide (i.e., 22 and 44 µL of N-Vinylformamide, abbreviated PHEMA/PNVF22 and PHEMA/PNVF44) prepared, then, 25 µL of TEMED was added, and the solution was dispensed into 5 mL plastic syringes after mixing (0.8 cm in diameter). Cryogel solutions were cooled to -18 °C and held there for 24 hours. After 24 h, the cryogel produced by free-radical polymerization was removed from the freezer. The cryogel was washed with distilled water for several hours to remove unreacted monomers. The same procedure described above synthesizes bare PHEMA cryogel without adding NVF monomer to ensure comparable results.

Characterization of cryogels

For the gelation efficiency (G) of the cryogels, the swollen cryogel sample was dried in a lyophilizer. After reaching the constant weight, the mass of the cryogel sample was determined, and the gelation efficiency was calculated using the following equation (Eq) (1):

$$G = \frac{w_D}{w_t} \times 100 \quad (\text{Eq) (1)}$$

According to equality, w_D is the dry weight of the cryogel, and w_t is the total mass of monomers in the polymerization mixture.

The dried cryogels (w_D , g) were soaked in deionized water at room temperature for 2 hours and roughly wiped with damp filter paper and weighed (w_1 , g). The cryogels were then subjected to mechanical compression to remove the water in the macropores and weighed again (w_2 , g). Then, the swelling degree (S.D.), swelling ratio (S.R.) and macroporosity (M) of the cryogels were calculated using the following equations (Eq) (2), (Eq) (3) and (Eq) (4), respectively:

$$S. D. = \frac{w_1}{w_D} \quad (\text{Eq) (2)}$$

$$S. R. = \frac{w_1 - w_D}{w_D} \times 100 \quad (\text{Eq) (3)}$$

$$M(\%) = \frac{w_1 - w_2}{w_2} \times 100 \quad (\text{Eq) (4)}$$

Dried cryogels were placed on the ATR (Nicolet iS10 ATR-FTIR, Thermo Scientific, Madison, WI, USA) probe and then FTIR spectra were obtained. The surface and pore morphology of cryogels scanning electron were analyzed with a microscope (SEM) (ZEISS GeminiSEM 500). Dried cryogels were coated with a molecular gold-palladium mixture on the SEM sample holder for 2 minutes, and then SEM images of the cryogels were obtained at various magnifications.

Determination of Yeast Cell Viability

The antifungal effects of the polymeric cryogels PHEMA/PNVF/22 and PHEMA/PNVF/44 were evaluated against wild type yeast strain of *Saccharomyces cerevisiae* BY4741 (MATa his3Δ1 leu2Δ0 met15Δ0 ura3Δ0). The PHEMA cryogel was used as control. The routine maintenance of the yeast cells was carried out on agar plates prepared with YPDA medium (10 g/L yeast extract, 20 g/L peptone, 20 g/L glucose and 20 g/L bactoagar, pH: 5.6) at 30 °C for 2 days. For the cytotoxicity assay, the cells were grown in YPD medium (10 g/L yeast extract, 20 g/L peptone and 20 g/L glucose, pH: 5.6) at 30 °C until their early-exponential phase (OD_{660nm}~0.5). Then, the cells were treated with the 0.15 gr of polymers at an initial concentration of 1x10⁷ CFU/mL for 24 h. After incubation period, the mediums were removed and the polymers were washed with the phosphate-buffered saline (PBS) with 150 rpm agitation for 1 h. The cell viability of the cells released to the washing solution was determined by Colony Forming Unit (CFU) assay. In the assay, 1 mL from the samples was taken and serially diluted in PBS. After the diluted samples were incubated at 30°C for 2 days, the appeared yeast colonies were counted to determine the percentage of CFU on PHEMA/PNVF/22 and PHEMA/PNVF/44 agar plates with respect to that on PHEMA control agar.

All the experiments were carried out in triplicate and the data are reported as the mean percentage of cell viability ± S.E.M. The differences in variance were analyzed statistically using a one-way analysis of variance (ANOVA) test by GraphPad Prism version 6.01 (GraphPad Software Inc.; La, Jolla, CA).

RESULTS AND DISCUSSION

Polymer analysis

The synthesized cryogels for this study (shown in Figure 1) have a spongy-elastic structure, an opaque appearance, and a cylindrical shape. PHEMA cryogels have an inter-network-like porous structure due to their crosslinking with MBAAm. This way, cryogels can uptake much water in this reticulated structure. The water in the pores of the polymer can be easily removed after any mechanical compression of the cryogel. On the other hand, when the dehydrated compressed cryogel piece is left to swell in the water again, it regains its original size within seconds. In addition, despite incorporating different concentrations of NVF monomer into PHEMA cryogels, no visible difference was detected in the optical images of the cryogels.

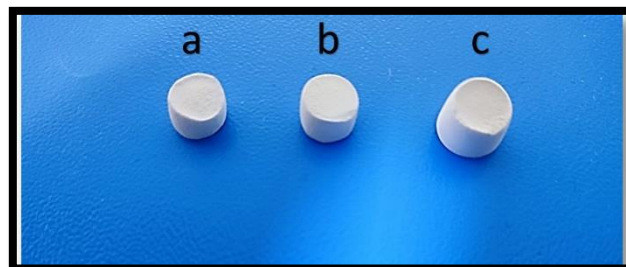


Figure 1. Optical images of cryogels: a) PHEMA, b) PHEMA/PNVF/22 and c) PHEMA/PNVF/44

The swelling behaviors of PHEMA, PHEMA/PNVF22, and PHEMA/PNVF/44 cryogels in water were investigated, and the results were given in Table 1. Accordingly, the swelling behavior of the PHEMA cryogels increased numerically with the concentration of the NVF monomer, which was added to the PHEMA structure as a copolymer. This can be explained by the hydrophilic nature of the NVF monomer, as well as by the increase in the number of pores that water can be absorbed in the polymer. On the other hand, the pore content and distribution of cryogels directly affect the activities in cell studies. For this reason, it is an easy-to-apply and fast-resulting method that can give an idea for the adhesion and proliferation of the cells of the cryogel, whose macroporosity is prepared. This study shows that the macroporosity of PHEMA cryogels containing NVF is higher than that of bare PHEMA cryogel, as can be seen from the macroporosity grade results in Table 1.

Table 1. Results for the swelling behaviour of cryogels

Cryogels	S.D.	S.R. (%)	M (%)	G
PHEMA	5.94	494.0	71.82	91.1
PHEMA/PNVF/22	6.11	511.72	71.04	92.1
PHEMA/PNVF/44	6.71	571.55	72.62	92.3

The infrared spectra of the PHEMA-based cryogels were shown in Figure 2. For PHEMA cryogel, the characteristic bands for PHEMA were observed at 3348 cm^{-1} (O-H stretching), 1709 cm^{-1} (C=O stretching), 1245.52 and 850.14 cm^{-1} (C-O and C-O-C stretching bands, respectively). Also (C-H) stretching bands were observed at 2948.75 cm^{-1} . These results are also compatible with previous literature studies (Bayrak et al. 2021). NVF, as a comonomer of HEMA-based cryogel (PHEMA/PNVF/44), was confirmed by the presence of the peak observed around 1244.58 cm^{-1} belonging to the C-N vibrations. The peaks at 1651 cm^{-1} and 1533 cm^{-1} indicated the Amide I and Amide II bonds, respectively. Given the proximity of the -OH and NH- peaks in FTIR spectra, it was assumed that the peak observed around 3287.86 cm^{-1} covered these two bands (Şarkaya and Allı, 2021a; Şarkaya et al., 2022).

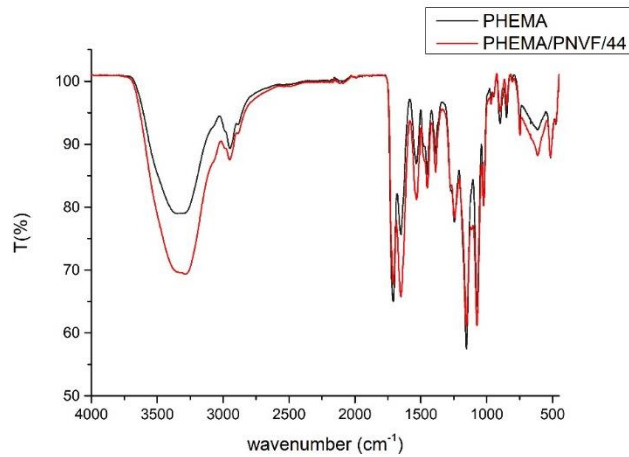


Figure 2. FTIR spectra of PHEMA and PHEMA/PNVF/44 cryogels

The porous morphological structure of the cryogels was investigated using field emission scanning electron microscopy (FE-SEM) in Figure 3. According to the images, there was no significant difference between the morphologies of the cryogels. Although all cryogels have highly porous structures, it was seen that the pores are not homogeneously distributed. This macroporous structure of cryogels is due to ice crystals. As a result of the melting of the ice crystals formed after the freezing reaction of the water molecules used as the solvent in the structure of the cryogels during the polymerization, a macroporous system associated with each other is formed. Cryogels' porous structure is important for cell attachment and the transport of residues or other specific species.

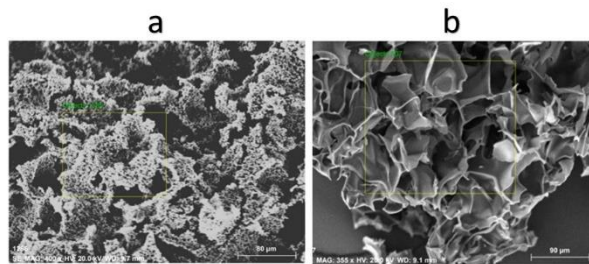


Figure 3. SEM images of PHEMA and PHEMA/PNVF44 cryogels

Antifungal Effects of PHEMA/PNVF Cryogels

In previous studies (Şarkaya and Allı, 2021b; Şarkaya et al., 2022), the characterizations of the cryogels were comprehensively studied. In addition, cytotoxicity tests of HEMA-based cryogels were also examined, and it was reported that they showed biocompatibility (Şarkaya et al. 2022). These results motivate us to investigate microbial activities of these cryogels. So, antifungal activities of PHEMA/PNVF cryogels are investigated against *S. cerevisiae* in this study.

The antifungal effects of PHEMA/PNVF polymers against *S. cerevisiae* yeast were presented at Figure 4. As can be seen from the results, PHEMA/PNVF polymers containing NVF in varying concentrations statistically significantly decreased yeast cell viability percentages compared to control group. PHEMA/PNVF/22 and PHEMA/PNVF/44 polymers effectively decrease cell proliferation to about %32 and 18, respectively. In current literature, there are some findings which shows the

antiproliferative activity of PNVF and its derivative poly(vinyl amine) (PVAm) against the pathogenic fungi *Candida albicans* ((Shandil et al., 2017; Sütekin et al., 2021; Demirci et al., 2022)). The main common result of these studies is that while PNVF shows moderate antifungal action, PVAm obtained from its acidic hydrolysis demonstrated much more potent antimicrobial activity against this pathogen. However, we have found that PNVF is quite effective on budding yeast *S. cerevisiae*. Although this yeast is not a pathogenic organism, it is accepted as an opportunistic species.

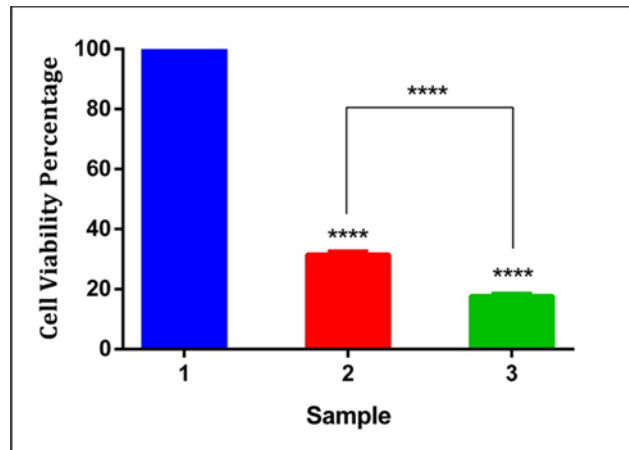


Figure 4. The viability percentages determined by CFU assay in yeast cells treated with PHEMA/PNVF/22 (2) and PHEMA/PNVF/44 (3) compared to the PHEMA control (1). Data with error bars show the mean \pm S.E.M of three experiments. ****= $p < 0.0001$ denote significant differences between control and other studied group or indicated groups by Tukey's multiple range tests.

Fungemia and other severe infections in the various systems of the body particularly in immunosuppressed or critically ill patients are the main issues with this organism (Muñoz et al., 2005; Dynowska et al., 2006; Algazaq et al., 2017). On the other hand, in a current study the skin infection caused by *S. cerevisiae* was described in an elderly. Additionally, the skin infection caused by *S. cerevisiae* was currently described in an elderly but immunocompetent person (Belmourida et al., 2021). So when our data are evaluated in the light of literature findings it would not be wrong to say that the antifungal effect of PNVF varies depending on the species. Although further studies are needed to elucidate its mechanism of action, its potential to be used as a wound-healing antifungal biomaterial should not be ignored.

CONCLUSION

In this study, bare PHEMA and PHEMA/PNVF cryogel series was prepared and characterized. The main goal of this study was to comparatively investigate of the antifungal activities of PHEMA/PNVF cryogels against *S. cerevisiae*. When the antifungal activities of these cryogels, which are known to be biocompatible, were evaluated, it was determined that PHEMA-NVF cryogels had higher antifungal effects than other HEMA-based cryogels. Within the scope of these results, the idea emerged that N-Vinylformamide additive PHEMA-based cryogels can be considered as a wound dressing material or antifungal drug loading systems against fungal infections in biotechnological fields. These studies could be updated with this idea following studies.

CONFLICT OF INTEREST

No conflict of interest was declared by the authors.

REFERENCES

- Ailincăi, D., Marin, L., Morariu, S., Mares, M., Bostanaru, A.C., Pinteala, M., Simionescu, B.C., Barboiu, M. (2016). Dual crosslinked iminoboronate-chitosan hydrogels with strong antifungal activity against *Candida* planktonic yeasts and biofilms. *Carbohydr Polym* 152, 306–316.
- Algazaq, J.N., Akrami, K., Martinez, F., McCutchan, A., and Bharti, A.R. (2017). *Saccharomyces cerevisiae* Laryngitis and Oral Lesions in a Patient with Laryngeal Carcinoma. *Case Rep Infect Dis* 2017, 1–4.

- Bayrak, G., Perçin, I., Kılıç Süloğlu, A., Denizli, A. (2021). Amino acid functionalized macroporous gelatin cryogels: Characterization and effects on cell proliferation. *Process Biochem* 110, 100–109.
- Belmourida, S., Palamino, H., Meziane, M., Ismaili, N., Benzekri, L., Hassam, B., Senouci, K. (2021). Skin infection with *Saccharomyces cerevisiae* in an immunocompetent patient: An exceptional infection. doi:10.7241/ourd.20214.30.
- Çetin, K., Denizli, A. (2019). Microcryogels as plastic antibodies for transferrin purification. *Process Biochem*, 79, 174–184.
- Coria-Hernández, J., Méndez-Albores, A., Meléndez-Pérez, R., Rosas-Mendoza, M.E., Arjona-Román, J.L. (2018). Thermal, Structural, and Rheological Characterization of Waxy Starch as a Cryogel for Its Application in Food Processing. *Polymers*, 10(4), 359.
- Demirci, S., Sütekin, S.D., Kurt, S.B., Güven, O., Sahiner, N. (2022). Poly(vinyl amine) microparticles derived from N-Vinylformamide and their versatile use. *Polym Bull*, 79(9), 7729–7751.
- Dragusin, D.M., Van Vlierberghe, S., Dubruel, P., Dierick, M., Van Hoorebeke, L., Declercq, H.A., Cornelissen, M.M., Stancu, I.C. (2012). Novel gelatin-PHEMA porous scaffolds for tissue engineering applications. *Soft Matter*, 8(37), 9589–9602.
- Dynowska, M., Roslan, M., Górska, K. (2006). *Saccharomyces cerevisiae* in the respiratory system, digestive system and on the skin in humans. *Acta Mycol*, 41(1), 139-144.
- Ferreira, F. V., Souza, L.P., Martins, T.M.M., Lopes, J.H., Mattos, B.D., Mariano, M., Pinheiro, I.F., Valverde, T.M., Livi, S., Camilli, J.A., Goes, A.M., Gouveia, R.F., Lona, L.M.F., Rojas, O.J. (2019). Nanocellulose/bioactive glass cryogels as scaffolds for bone regeneration. *Nanoscale*, 11(42), 19842–19849.
- García-Millán, E., Koprivnik, S., Otero-Espinar, F.J. (2015). Drug loading optimization and extended drug delivery of corticoids from pHEMA based soft contact lenses hydrogels via chemical and microstructural modifications. *Int J Pharm*, 487(1–2), 260–269.
- García-Uriostegui, L., Delgado, E., Meléndez-Ortiz, H.I., Camacho-Villegas, T.A., Esquivel-Solís, H., Gatenholm, P., Toriz, G. (2018). Spruce xylan/HEMA-SBA15 hybrid hydrogels as a potential scaffold for fibroblast growth and attachment. *Carbohydr Polym*, 201, 490–499.
- Karacan, P., and Okay, O. (2013). Ethidium bromide binding to DNA cryogels. *React Funct Polym*, 73(3), 442–450.
- Lozinsky, V. (2018). Cryostructuring of Polymeric Systems. 50.† Cryogels and Cryotropic Gel-Formation: Terms and Definitions. *Gels*, 4(3), 77.
- Luo, W., Wang, L., Feng, R., Zhao, C., Wang, J., Cai, T. (2021). Preparation of composite anion exchange membranes based on in-situ copolymerization of N-vinyl formamide and divinylbenzene in porous PTFE. *J Appl Polym Sci*, 138(8), 49872.
- Manzoor, A., Dar, A.H., Pandey, V.K., Shams, R., Khan, S., Panesar, P.S., Kennedy, J.F., Fayaz, U., Khan, S.A. (2022). Recent insights into polysaccharide-based hydrogels and their potential applications in food sector: A review. *Int J Biol Macromol*, 213, 987–1006.
- McFarland, L. V. (2010). Systematic review and meta-analysis of *Saccharomyces boulardii* in adult patients. *World J Gastroenterol*, 16(18), 2202.
- Moghadam, M.N., Pioletti, D.P. (2016). Biodegradable HEMA-based hydrogels with enhanced mechanical properties. *J. Biomed. Mater. Res. Part B Appl Biomater*, 104(6), 1161–1169.
- Muñoz, P., Bouza, E., Cuenca-Estrella, M., Eiros, J.M., Pérez, M.J., Sánchez-Somolinos, M., Rincón, C., Hortal, J., Peláez, T. (2005). *Saccharomyces cerevisiae* fungemia: An emerging infectious disease. *Clin Infect Dis*, 40(11), 1625–1634.
- Nash, A.K., Auchtung, T.A., Wong, M.C., Smith, D.P., Gesell, J.R., Ross, M.C., Stewart, C.J., Metcalf, G.A., Muzny, D.M., Gibbs, R.A., Ajami, N.J., Petrosino, J.F. (2017). The gut mycobiome of the Human Microbiome Project healthy cohort. *Microbiome*, 5(1), 153.

- Roointan, A., Farzanfar, J., Mohammadi-Samani, S., Behzad-Behbahani, A., Farjadian, F. (2018). Smart pH responsive drug delivery system based on poly(HEMA-co-DMAEMA) nanohydrogel. *Int J Pharm*, 552(1–2), 301–311.
- Şarkaya, K., Akıncioğlu, G., Akıncioğlu, S. (2022). Investigation of tribological properties of HEMA-based cryogels as potential articular cartilage biomaterials. doi:10.1080/25740881.2022.2039190.
- Şarkaya, K., Allı, A. (2021). Synthesis and characterization of cryogels of p(HEMA-N-vinylformamide) and p(HEMA-N-Vinylpyrrolidone) for chemical release behaviour. *J Porous Mater*, 28(3), 853–865.
- Şarkaya, K., Bakhshpour, M., Denizli, A. (2018). Ag⁺ ions imprinted cryogels for selective removal of silver ions from aqueous solutions. *Sep Sci Technol*, 1–12
- Sevgül Bakay, M., Şarkaya, K., Çadırcı, M. (2022). Electrical properties of CsPbX₃ (X=Cl, Br) perovskite quantum dot/poly(HEMA) cryogel nanocomposites. *Mater Chem Phys*, 277, 125479.
- Shandil, Y., Dautoo, U.K., Chauhan, G.S. (2017). New modified poly(vinylamine)-gels as selective and efficient Hg²⁺ ions adsorbents. *Chem Eng J* 316, 978–987.
- Shi, L., Khondee, S., Linz, T.H., Berkland, C. (2008). Poly(N-vinylformamide) nanogels capable of pH-sensitive protein release. *Macromolecules*, 41(17), 6546–6554.
- Shih, T.Y., Blacklow, S.O., Li, A.W., Freedman, B.R., Bencherif, S., Koshy, S.T., Darnell, M.C., Mooney, D.J. (2018). Injectable, Tough Alginate Cryogels as Cancer Vaccines. *Adv Healthc Mater* 7(10), 1701469.
- Su, E., and Okay, O. 2019. Cryogenic formation-structure-property relationships of poly (2-acrylamido-2-methyl-1-propanesulfonic acid) cryogels. *Polymer (Guildf) Elsevier*.
- Suekama, T.C., Aziz, V., Mohammadi, Z., Berkland, C., Gehrke, S.H. (2013). Synthesis and characterization of poly(N-vinyl formamide) hydrogels—A potential alternative to polyacrylamide hydrogels. *J Polym Sci, Part A Polym Chem*, 51(2), 435–445.
- Sütekin, S.D., Demirci, S., Kurt, S.B., Güven, O., Sahiner, N. (2021). Tunable fluorescent and antimicrobial properties of poly(vinyl amine) affected by the acidic or basic hydrolysis of poly(N-vinylformamide). *J Appl Polym Sci*, 138(42), 51234.
- Veiga, A.S., Schneider, J.P. (2013). Antimicrobial hydrogels for the treatment of infection. *Biopolymers*, 100(6), 637–644.
- Zhao, X., Wu, H., Guo, B., Dong, R., Qiu, Y., Ma, P.X. (2017). Antibacterial anti-oxidant electroactive injectable hydrogel as self-healing wound dressing with hemostasis and adhesiveness for cutaneous wound healing. *Biomaterials*, 122, 34–47.
- Zumbuehl, A., Ferreira, L., Kuhn, D., Astashkina, A., Long, L., Yeo, Y., Iaconis, T., Ghannoum, M., Fink, G.R., Langer, R., Kohane, D.S. (2007). Antifungal hydrogels. *Proc Natl Acad Sci*, 104(32), 12994–12998.